The temperature dependence of magnetic losses in CoO-doped Mn-Zn ferrites

The temperature dependence of magnetic losses in CoO-doped Mn-Zn ferrites

Cinzia Beatrice[1b], Samuel Dobák[2a], Vasiliki Tsakaloudi[3], Carlo Ragusa[4], Fausto Fiorillo[1]

[1]*Advanced Materials Metrology and Life Science Division, Istituto Nazionale di Ricerca Metrologica INRIM, 10135 Torino, Italy*

[2]*Institute of Physics, P.J. Šafárik University, 04167 Košice, Slovakia.*

[3]*Laboratory of Inorganic Materials, CERTH, 57001 Thermi-Thessaloniki, Greece.*

[4] *Energy Department, Politecnico di Torino, 10129 Torino, Italy.*

CoO-doping is known to stabilize the temperature dependence of initial permeability and magnetic losses in Mn-Zn ferrites, besides providing, with appropriate dopant contents, good soft magnetic response at and around room temperature. These effects, thought to derive from the mechanism of anisotropy compensation, are, however, poorly assessed from a quantitative viewpoint. In this work, we overcome such limitation by providing, besides extensive experimental investigation versus frequency (DC – 1 GHz), CoO content ($0 \leq$ CoO ≤ 6000 ppm), and temperature (-20 °C $\leq T \leq$130 °C) of permeability and losses of sintered Mn-Zn ferrites, a comprehensive theoretical framework. This relies on the separate identification of domain wall motion and moment rotations and on a generalized approach to magnetic loss decomposition. The average effective anisotropy constant $\langle K_{\mathrm{eff}} \rangle$ is obtained and found to monotonically decrease with temperature, depending on the CoO content. The quasi-static energy loss W_{h} is then predicted to pass through a deep minimum for CoO = 3000 - 4000 ppm at and below the room temperature, while becoming weakly dependent on CoO under increasing T. The rotational loss $W_{\mathrm{rot}}(f)$ is calculated via the complex permeability, as obtained from the Landau-Lifshitz equation for distributed values of the local effective anisotropy field $H_{\mathrm{k,eff}}$ (i.e. ferromagnetic resonance frequency). Finally, the excess loss $W_{\mathrm{exc}}(f)$ is derived and found to comply with suitable analytical formulation. It is concluded that, by achieving via the rotational permeability value and behavior of the magnetic anisotropy constant, we can predict the ensuing properties of hysteresis, excess, and rotational losses.

---

[a]This research was performed while S. Dobák was at the Advanced Materials Metrology and Life Science Division of INRIM, Torino, Italy, under grant from the National Scholarship Program of the Slovak Republic.
[b]Author to whom correspondence should be addressed: c.beatrice@inrim.it.

I. INTRODUCTION

Sintered Mn-Zn ferrite is the material of choice for the inductive components used in power electronics. Its good soft magnetic properties, descending from solidly assessed preparation methods and relying on well-known chemical and structural properties, permit one to usefully cover a very large range of frequencies. This provides for widespread applications in an array of devices, like switch-mode power supplies, buck converters, inverters, pulse transformers. Fine chemistry of additives is crucial to the optimization of the Mn-Zn ferrite properties,[1,2] because of the role these can have in influencing grain growth and microstructure[1] and in regulating the magnetic anisotropy through the mechanism of anisotropy compensation[3], besides affecting the resistivity of the grains and the grain boundaries by solute cations and segregated second phases.[4,5] Thus, oxides segregating at grain boundaries, like CaO, V_2O_5, Nb_2O_5, and SiO_2, can favor densification kinetics and increase the grain boundary resistivity.[6] At the same time, by regulating excess Fe^{2+} cations via Fe_2O_3 stoichiometry or appropriate partial pressure of oxygen during sintering, one can achieve balanced effects between increased magnetic softening by anisotropy compensation and decreased grain resistivity[7,8]. With appropriate contents of the positive anisotropy of Fe^{2+} ions, combining with the negative anisotropy of the host lattice, minimum loss value is attained at temperatures T = 80 – 100 °C, the typical working temperatures of the inductive components used in power electronics. The variation of the magnetic loss with temperature can indeed be relevant, with the energy loss under standard regimes (e.g., 100 mT peak induction at 100 kHz) decreased by a factor 2-3 and the initial permeability increased by a similar factor on passing from room temperature to the optimal working temperature.[7,9-11] But modern applications in such diverse fields as solar energy conversion or automotive electronics require high and uniform component efficiency on a relatively wide range of temperatures, a performance achievable, for example, with the thermomagnetically treated nanocrystalline tapewound cores.[12] These are competitive materials, which can overcome soft ferrites in most applications, though at higher costs.

A standard way to address the temperature dependence of magnetic properties in Mn-Zn ferrites is one of introducing a suitable amount of Co^{2+} cations, where, besides the typical abovementioned oxides, CoO is added to the pre-fired powders.[9,11, 13-15] The temperature dependent compensation of the negative anisotropy of the host Fe^{3+} ions by the positive Co^{2+} ions is the mechanism responsible, with appropriate Co^{2+} concentration, for the smoothing out of the loss and permeability dependence on temperature. At present time, however, actual value and behavior of the effective average anisotropy constant $<K_{eff}>$, the quantity lying behind the features of the magnetization process, are loosely guessed at best in the literature. By talking of effective magnetic anisotropy, we take into account, besides the magnetocrystalline and induced anisotropies, the magnetostatic contribution deriving from local divergence of the magnetization, namely at grain boundaries and pores.

We have recently shown that an estimate of $<K_{eff}>$ can be made in sintered ferrites, by extracting the contribution of the rotational magnetization processes from the value of the low-field DC permeability.[16] Applied to the present experiments on Co-doped Mn-Zn ferrites, this feat permits us to verify that optimal addition of CoO = 3000 – 4000 ppm leads to smoothed dependence of $<K_{eff}>$ on T and, correspondingly, to a stable behavior versus temperature of initial permeability and energy loss, from DC to the deep MHz range. By determining the matrix of $<K_{eff}>$ (CoO, T) values we are eventually able to predict the dependence of the quasi-static (hysteresis) energy loss W_h on the CoO content at different temperatures and proceed to the analysis of the broadband dynamic loss. This is done according to the basic statements of the Statistical

Journal of Applied Physics

Theory of Losses (STL), which are extended to cover the loss phenomenology over a very large range of frequencies in the insulating/semi-insulating sintered ferrites.[16,17] In this way we overcome the limited predicting ability of the standard approach to the energy losses in Mn-Zn ferrites, based on the identification and combination of quasi-static W_h, eddy-current W_e, and residual W_r losses.[10,14,18,19] Of these components, only W_e is calculated, in general, making use of a classical maxwellian formulation and neglecting the actual structural and magnetic heterogeneity of the material. By the generalized STL, we provide a comprehensive interpretative framework, where, while accounting for the actual heterogeneous structure of the sintered ferrites, we recognize the separate contributions of domain wall (dw) displacements and rotations to the magnetization process, with the associated dissipation channels provided by eddy currents and spin damping.[16,17,20]

In this work we have investigated the temperature dependence of the magnetic properties of Mn-Zn ferrites obtained by sintering at T = 1325 °C, subjected to conventional doping by CaO and Nb_2O_5 and additional doping by CoO, in quantities ranging between 0 and 6000 ppm. Permeability and energy losses have been measured, at different values of the peak polarization J_p, up to 1 GHz and at temperatures ranging between – 20 °C and 130 °C. The eddy current dissipation channel is easily identified and the related loss contribution $W_{cl,eddy}$ is singled out by means of broadband loss measurements on progressively thinned ring samples, as illustrated in the example of Fig. 1, regarding CoO = 3000 ppm doped ring samples, tested at different temperatures. We see in this figure that, on passing from the 4.97 mm thick to the 1.30 mm thick ring samples, $W(f)$ remains unchanged below about 4 MHz, signaling corresponding negligible $W_{cl,eddy}$. The difference appearing at the highest frequencies is what we expect from the equation for the classical eddy current loss at high frequencies in samples of rectangular cross-section

$$W_{\mathrm{cl,eddy}}(J_\mathrm{p}, f) = \left(\frac{\pi^2}{6}\right)\sigma'(f)\cdot(12k(R)S)J_\mathrm{p}^2 f \quad , \qquad [\mathrm{J/m^3}] \qquad (1)$$

where $\sigma'(f)$ is the real part of the measured conductivity and $k(R)$ is an increasing function of the aspect ratio R of the cross-section of area S. It is given by $k(R) = 0.0744R - 0.0434R^2$ and saturates, for R = 1, at the value $k(R)$ = 0.035.[21] It turns out that $W_{cl,eddy}$ can be neglected in the thinner sample. It is remarked that Eq. (1) can be applied at high frequencies, because the capacitive grain boundary layers are virtual short circuits and the material electrically behaves as a continuum.[22,23]

Having previously estimated $\langle K_{eff}\rangle$ by knowledge of the DC rotational permeability, a quantity basically independent of J_p in the Rayleigh region, we are consistently guided to the calculation of the real $\mu'_{rot}(f)$, and imaginary $\mu''_{rot}(f)$ rotational permeabilities versus frequency as solutions of the Landau-Lifshitz equation. From the theoretical $\mu'_{rot}(f)$ and $\mu''_{rot}(f)$ we immediately obtain the rotational loss by spin damping

$$W_{\mathrm{rot}}(J_\mathrm{p}, f) = \pi J_\mathrm{p}^2 \mu''_{\mathrm{rot}}(f)/(\mu'^2(f) + \mu''^2(f)) \quad , \qquad (2)$$

which applies to the experimental loss curves of the thin eddy-current-free samples. With $W_h(J_p)$ and $W_{rot}(J_p, f)$ available, the excess loss $W_{exc}(J_p, f)$, the dissipative term directly related to the viscous motion of the dws, is obtained as $W_{exc}(J_p, f) = W(f) - W_h(J_p) - W_{rot}(J_p, f)$. It will be shown that the ultimate effect of the smoothed dependence of $\langle K_{eff}\rangle$ on temperature ensuing from the addition of CoO = 3000 – 4000 ppm is one of improving the temperature stability of all the loss components, be these related to dw displacements or rotations. The involved dissipation mechanism is chiefly one of spin damping, that is, decay of the precessional spin motion into lattice vibrational modes, the contribution of eddy currents possibly adding at very high frequencies in sufficiently large samples.

II. EXPERIMENTAL METHOD AND PROCEDURE

Mn-Zn ferrite powders were prepared from high-purity raw materials by dry mixing 72% Fe_2O_3, 21.60 % MnO and 6.35% ZnO and prefiring at 850 °C in air. The prefired powders were doped under a defined doping scheme with CaO and Nb_2O_5 and further addition of CoO in concentrations ranging between 0 – 6000 ppm, step 1000 ppm. As described in detail in Ref.[24], ring specimens of outside diameter about 14 mm were obtained by compaction of the milled and granulated powders. Sintering of the samples was made at T = 1325 °C, under appropriate partial oxygen pressure, followed by microstructural analysis by Scanning Electron Microscopy (JEOL 6300) and density measurement by Archimedes' method. The average grain size ranged between 10.7 μm and 13.1 μm and the density slightly increased from 4920 kg/m^3 (CoO = 0) to 5040 kg/m^3 (CoO = 6000 ppm). The real ρ'(f) and imaginary ρ'' (f) resistivity components were obtained by the standard four-point electrical impedance measurements up to f = 20 MHz. The found dependence of ρ'(f) and ρ''(f) on frequency is consistent with the conventional equivalent RC circuit lumping the electrical properties of the semiconducting grains and their insulating layer.[22] The DC (grain boundary layer) and high-frequency (grain interior) resistivities are moderately affected (up to 20 – 30 %) by CoO doping, with ρ''(f) becoming negligible with respect to ρ'(f) beyond about 20 MHz. At such frequencies, the conductivity in Eq. (1) $\sigma'(f) = \frac{\rho'(f)}{\rho'(f)^2+\rho''(f)^2} \sim \frac{1}{\rho'(f)}$ becomes quite constant and little dependent on temperature, as shown in the example of Fig. 2. The DC resistivity, on the contrary, falls by more than one order of magnitude on passing from 0 °C to 120 °C, without affecting the loss behavior. Based on the measured $\rho'(f)$ and Eq. (1), the eddy current loss component is calculated at high frequencies, resulting in the $W_{\mathrm{cl,eddy}} \propto f$ curves shown in Fig. 1 (large symbols), whose behaviors are consistent with the difference found between the measured $W(f)$ in the 4.97 mm and 1.30 mm thick samples.

The Mn-Zn ferrite ring samples, having outside and inside diameters around 14 mm and 9 mm, respectively, were magnetically characterized under sinusoidal induction at defined values of the peak polarization J_p, up to the maximum frequency of 10 MHz, by means of a calibrated hysteresisgraph-wattmeter. The saturation (spontaneous) polarization J_s was obtained by measuring the upper portion of the magnetization curve, up to applied field H of few kA/m, and extrapolation of J vs. $1/H \rightarrow 0$. Measurements above room temperature were made by keeping the sample inside a nylon holder, surrounded by a dc-supplied non-inductive heater and by detecting the sample temperature by means of a copper-constantan micro-thermocouple stuck on the sample surface. The measurements below room temperature were made by dipping the sample in the bath of a PolyScience PP15R-40-A12E programmable cryostat.

The fluxmetric measurements overlapped, starting from a few hundred kHz, with transmission line measurements, performed up to 1 GHz through a Rohde&Schwarz ZNB8 Vector Network Analyzer (VNA). By the latter setup one could cover the upper range of frequencies at fixed 10 mW exciting power. The detailed measuring procedure is discussed in Refs. [17, 25], but we remark here that we can reconcile the VNA results, where J_p is small (few mT at most) and decreasing under increasing frequencies, with the fluxmetric measurements, taken at defined J_p value. The experiments actually show that at sufficiently high frequencies, μ'(f) and μ''(f) in Mn-Zn ferrites become independent of J_p and the energy loss is directly obtained at any J_p value as $W(J_p, f) = \pi J_p^2 \mu''(f)/(\mu'^2(f) + \mu''^2(f))$. We see for example in Fig. 1 how $W(f)$, fluxmetrically measured at J_p = 50 mT (symbols), seamlessly extends beyond about 2 MHz into the quantity calculated from the VNA measured μ'(f) and μ''(f) and the previous equation (continuous and dashed lines). The inset in the same

figure shows that at the very low value J_p = 2 mT the fluxmetric and VNA-derived $W(f)$ curves start to overlap at the frequency f_o ~ 600 kHz, according to concurrent overlapping of $\mu'(f)$ and $\mu''(f)$. Of course, by increasing J_p, that is, increasing the dw contribution $J_{p,dw}$, f_o moves toward higher values. Because of the experimental limits of the fluxmetric method, regarding available exciting power and sample overheating, f_o is found for J_p higher than some 50 mT by reasonable extrapolation of the fluxmetric $W(f)$ curves.[24] The reason for the ultimate high-frequency coalescence of the $W(f)$ curves at defined high J_p values with the curves calculated through the VNA measurements lies in the earlier relaxation of $\mu_{dw}(f)$ with respect to $\mu_{rot}(f)$, whatever the dissipation mechanism (i.e., either eddy currents or spin damping). If we compare, in particular, the viscous dynamics of the magnetic moments inside the moving walls and inside the domains and we consider the related frictional torque, expressed, according to the Gilbert equation, as

$$|\boldsymbol{\Gamma}| = \left(\frac{\alpha}{\gamma\mu_0 J_s}\right)\left|\boldsymbol{J}\times\frac{\mathrm{d}\boldsymbol{J}}{\mathrm{d}t}\right| = \left(\frac{\alpha}{\gamma\mu_0}\right)J_s\frac{\mathrm{d}\theta}{\mathrm{d}t} \quad , \tag{3}$$

where α is the damping constant, γ is electron gyromagnetic ratio, and $\mathrm{d}\theta/\mathrm{d}t$ is the angular velocity of the rotating spins, we realize that much larger Γ is associated with the dw motion. Consequently, rotations will increasingly be favored by increasing the magnetizing frequency and, when this is sufficiently high, $\mu_{dw}(f)$ will become sufficiently small with respect to $\mu_{rot}(f)$, the magnetic constitutive equation will generally tend to linear behavior, and $W(f)$ will be determined, also at relatively high J_p values, using the VNA determined $\mu'(f)$ and $\mu''(f)$.

III. INITIAL PERMEABILITY, MAGNETIC LOSSES, AND ANISOTROPY CONSTANT VERSUS TEMPERATURE

The acknowledged main role of Co^{2+} ions in Mn-Zn ferrites is one of introducing a uniaxial magnetic anisotropy, which, in combination with the native anisotropy associated with the Fe^{3+} and Fe^{2+} ions, can stabilize the magnetic properties with temperature in the useful range 23 °C – 100 °C. In the present work, we show that the related phenomena are susceptible of a quantitative assessment. This is based on the analysis of the magnetization process and its description in terms of rotational and dw contributions and the identification of the related dissipation mechanisms. The examples of measured initial dc permeability μ_i and quasi-static energy loss W_h (J_p = 50 mT) versus temperature in doped and undoped materials, as provided in Figs. 3 and 4, show that CoO doping at concentrations of 3000 – 4000 ppm is effective in smoothing out both the $W(f)$ and μ_i dependence on T. The overall dependence of $W(f)$ on T at different frequencies, shown up to 100 MHz in Fig. 5, additionally puts in evidence, in accordance with the results given in Fig. 1, that on entering the MHz range little effect of temperature is observed and the $W(f)$ vs. T curves obtained with different CoO contents tend to coalesce. To note that we deal here with general behaviors, quite independent of the specific J_p value. They point to the remarkable role of the anisotropy contribution by the Co^{2+} ions, an effect frequently stressed in the literature and justified on qualitative grounds only. We demonstrate in the following that the average effective anisotropy $\langle K_{eff}\rangle$ and its dependence on CoO and temperature can be estimated and their role on the broadband behavior of the energy loss consistently verified.

Journal of Applied Physics

AIP Publishing

The starting point of our analysis consists in separating the rotational and domain wall processes. These are inevitably concurring mechanisms in Mn-Zn ferrites, because of the very low level of the magnetocrystalline anisotropy, in contrast, for example, with the unfolding of the magnetization reversal in soft magnetic steels. We take thus advantage of two basic features: 1) The quasi-static imaginary permeability is exclusively associated with the dw displacements (i.e., the quasi-static loss): $\mu''(f \to 0) \equiv \mu''_{dw}(f \to 0)$; 2) The rotational permeability is to good approximation independent of J_p, up to J_p = 50 - 100 mT (the increase of the dc permeability with J_p being exclusively due to the dw displacements). It turns out, for example, that by making the difference μ''(50 mT) - μ''(2 mT) = μ''_{dw}(50 mT) - μ''_{dw} (2 mT) ~ μ''_{dw}(50 mT), only a dw related term is obtained. As fully discussed in Ref.[16], these conditions lead, by means of a self-consistent argument, to the derivation of $\mu''_{rot}(f)$ and $\mu'_{rot}(f)$. Fig. 6 provides an example of the so-found permeability decomposition, where the resonant character of $\mu'_{rot}(f)$ and its large prevalence with respect to $\mu'_{dw}(f)$ at J_p = 10 mT and J_p = 50 mT are appreciated. A Lorentzian-like behavior, pointing to a relaxation mechanism, is exhibited by the $\mu'_{dw}(f)$ spectrum. It is concluded that the value of the initial permeability and its dependence on temperature, shown in Fig. 3, are very close to those of the rotational permeability.

We associate now with any direction in the half-space an average value of the effective anisotropy constant $<K_{eff}>$ and we write the related rotational dc susceptibility (small rotations) for any angle θ made with the applied field as $\chi_{rot}(\theta) = \frac{J_s^2}{2\mu_0 <K_{eff}>} \cdot sin^2(\theta)$, which, once integrated over the different orientations, provides for the dc rotational permeability $\mu_{rot,dc} \cong \mu'_{rot,dc}$

$$\mu_{rot,dc} = 1 + \frac{J_s^2}{3\mu_0 <K_{eff}>} \quad , \tag{4}$$

making it possible to estimate $<K_{eff}>$ and its dependence on CoO doping and temperature by measuring $\mu_{rot,dc}$. We thus arrive at the full matrix of values $<K_{eff}>$(CoO, T) shown in Fig. 7. The mechanism of anisotropy compensation is such as to make $<K_{eff}>$ least dependent on temperature for CoO = 3000 ppm and little dependent on CoO doping beyond some 100 °C. We can qualitatively compare the similar trends of $<K_{eff}>(T)$ in Fig. 7a and $W_h(T)$ in Fig. 4, to bring forth the connection between these two quantities. More specifically, we can make a quantitative estimate of it, for any J_p value, by considering the coercive field H_c and its relationship with $W_h(J_p)$, according to $W_h(J_p) \cong 4\, H_c\, J_{p,dw}$, with $J_{p,dw} = \frac{\mu_{dw,dc}}{\mu_{dw,dc}+\mu_{rot,dc}} J_p$ the dw contribution to J_p. We can write, on general grounds, the coercive field as $H_c = a(J_p)\frac{\gamma_w}{J_s <s>}$, where $\gamma_w = 2\sqrt{A < K_{eff} >}$ is the specific dw energy (J/m^2), A ~ 10^{-11} J/m is the stiffness constant, $<s>$ is the average grain size, and $a(J_p)$ is a parameter accounting for the increase of the coercive field with J_p, that is, for the distribution of the local pinning field strength. We thus obtain for given J_p

$$W_h(J_p) = 8a(J_p)\sqrt{A}\frac{\sqrt{<K_{eff}>}}{J_s <s>} \cdot \frac{\mu_{dw,dc}}{\mu_{dw,dc}+\mu_{rot,dc}} J_p \quad , \tag{5}$$

where J_s and $<s>$ are experimentally known and $<K_{eff}>$, $\mu_{dw,dc}$, and $\mu_{rot,dc}$ are all obtained from the previously discussed analysis of permeability. By this expression, we describe the dependence of $W_h(J_p)$ on the CoO content and the way it modifies with temperature, as illustrated in Fig. 8 and Fig. 9. The fitting parameter $a(J_p)$ is observed to follow a quasi-linear dependence on J_p, typical of $H_c(J_p)$ in polycrystalline materials, eventually resulting, because of the increase of the ratio $\mu_{dw,dc}/\mu_{rot,dc}$ with J_p, in the power law $W_h(J_p) \propto J_p^n$, with $n > 2$. We are thus able to predict the passage of W_h through a deep minimum corresponding to CoO = 3000 – 4000 ppm, around and below room temperature and its evolution into moderate near-monotonic decrease with CoO upon increasing temperatures.

IV. ENERGY LOSS VERSUS FREQUENCY AND TEMPERATURE AND ITS PREDICTION

Having assessed the role of temperature on the quasi-static energy loss $W_h(J_p)$, we turn our attention to the overall $W(f)$ behavior and the way we can consistently predict results like the ones reported in Fig. 1 and Fig. 5, where the challenge posed by dealing with a very large bandwidth, covering the material properties up to negligible magnetic response (see Fig. 6), compounds with the phenomena associated with changing temperatures. We then need to provide a theoretical framework for the dynamic loss in a physical context quite different from the usual case of polycrystalline steel sheets. We have to deal, for example, with important rotational processes and low-to-negligible electrical conductivity, and dominant spin-damping dissipation mechanism. But we actually have all the ingredients for a generalization of the STL to non-conducting soft magnets: a stochastic sequence of elementary magnetization reversals generating the hysteresis loss component W_h, a distribution of local coercive fields, and the proportional relationship between the dynamic viscous field and the velocity of the moving wall, as experimentally proved in insulating ferrite monocrystals.[26] We can write, in particular, for a wall travelling at speed $\dot{x}$ in the magnetic medium under the pressure applied by the field H

$$(\beta_{eddy} + \beta_{sd})\dot{x} = 2J_s(H - H_c)\ , \qquad (6)$$

where β_{eddy} and β_{sd} are the eddy current and spin damping coefficients, respectively, and H_c is the threshold field. This is in essence, with $\beta_{eddy} >> \beta_{sd}$, the base equation on which the STL for steel sheets is built.[27] In our case, we have, according to the STL, $\beta_{eddy} = 4\sigma J_s^2 G<s>$, with $G = 0.1356$ and σ the conductivity of the grain (i.e. the conductivity of the material at high frequencies, see Fig. 2) and $\beta_{sd} = (2J_s/\mu_0\gamma\delta)\cdot\alpha$, with δ the dw thickness. It turns out that in the Mn-Zn ferrites $\beta_{eddy} << \beta_{sd}$ [17] and spin damping can be taken as the sole significant dissipation mechanism for the moving domain walls. We can then conclude that the dw generated dynamic loss in Mn-Zn ferrites can be given fairly similar treatment as in steel sheets, but for the involved damping mechanism, and one can still invoke the statistical properties of the local coercive fields in regulating the unfolding of the dw processes under increasing magnetizing frequencies. It is nevertheless fair to say that, as shown in Fig. 1, the combination of very high frequencies and large sample size can give rise to some eddy current loss contribution, associated with the current patterns no more confined within the grains and investing the whole sample cross-section (classical loss). But we can either calculate this contribution[23] or straightforwardly get rid of it, as shown in the same figure, by sample thinning.

The previous discussion guides us toward a predicting approach of the dynamic loss $W_{dyn}(f)$, by which we assess the whole phenomenology presiding over the measured many orders of magnitudes increase of $W(f)$, from the limiting irreducible value W_h in the limit $f \to 0$ to the radiofrequency regime. Since we have previously shown that we can

Journal of Applied Physics

AIP Publishing

distinguish between the separate contributions to the magnetization reversal provided by rotations and dw displacements, we can equally identify different loss contributions. It is generally observed that the quasi-linear assumption provides an excellent approximation of the actual dynamic loops up to relatively high J_p values (say at least 100 mT in typical Mn-Zn ferrites)[23] and we write $W(J_p, f)$ as

$$W_{\mathrm{dyn}}(J_{\mathrm{p}}, f) = \frac{\pi J_{\mathrm{p}}^2\left(\mu''_{\mathrm{dw}}(f) + \mu''_{\mathrm{rot}}(f)\right)}{\mu'^2(f) + \mu''^2(f)} = W_{\mathrm{exc}}(J_{\mathrm{p}}, f) + W_{\mathrm{rot}}(J_{\mathrm{p}}, f) \quad , \tag{7}$$

where we have defined with $W_{\mathrm{exc}}(J_{\mathrm{p}}, f)$ the dw-related dynamic losses. On the other hand, the rotational process finds an analytical description by the linear Landau-Lifshitz equation and its solution in terms of $\mu'_{\mathrm{rot}}(f)$ and $\mu''_{\mathrm{rot}}(f)$. We have described in detail in previous papers[17,25] the assumptions and calculations by which one can eventually express the relative rotational permeability components as

$$< \mu'_{\mathrm{rot}}(f) > = 1 + \frac{2}{3}\int_0^{\infty} g(H_{\mathrm{k,eff}})\, \chi'_{\mathrm{rot}}\left(f, H_{\mathrm{k,eff}}, \frac{\pi}{2}\right) \mathrm{d}H_{\mathrm{k,eff}} \tag{8}$$

$$< \mu''_{\mathrm{rot}}(f) > = \frac{2}{3}\int_0^{\infty} g(H_{\mathrm{k,eff}})\, \chi''_{\mathrm{rot}}\left(f, H_{\mathrm{k,eff}}, \frac{\pi}{2}\right) \mathrm{d}H_{\mathrm{k,eff}} \quad , \tag{9}$$

resulting from averaging with respect to amplitude and orientation distribution of the effective anisotropy field $H_{\mathrm{k,eff}} = 2K_{\mathrm{eff}}/J_{\mathrm{s}}$. A lognormal distribution $g(H_{\mathrm{k,eff}})$ is assumed,

$$g(H_{\mathrm{k,eff}}) = \frac{1}{\sqrt{2\pi}\lambda H_{\mathrm{k,eff}}} \cdot \exp\left[-\frac{(ln(H_{k,eff}) - h)^2}{2\lambda^2}\right] \quad , \tag{10}$$

where $h = <\ln(H_{\mathrm{k,eff}})>$ and λ is the standard deviation of $\ln(H_{\mathrm{k,eff}})$. $< H_{\mathrm{k,eff}} >$ descends from the $<K_{\mathrm{eff}}>$ value obtained by extracting the rotational permeability (see Fig. 6). Fig. 10a provides an example of the measured $\mu'(f)$ and $\mu''(f)$ behaviors at J_p = 50 mT in a CoO = 3000 ppm doped ferrite, with the derived rotational components $\mu'_{\mathrm{rot}}(f)$ and $\mu''_{\mathrm{rot}}(f)$ and their fitting by Eqs. (8) and (9). Besides the value of the damping constant α = 0.04, a lower limit H_{k0} for the admissible anisotropy fields is assumed. To note that $g(H_{\mathrm{k,eff}})$ becomes frequency dependent at very high frequencies. In particular, the constant C (reported in Fig. 10a) provides a measure of the drift of the distribution $g(H_{\mathrm{k,eff}})$ towards increasingly high $H_{\mathrm{k,eff}}$ values beyond a few MHz, where an increasing number of grains pass through resonance and become transparent to the ac field.[25] The phenomenology of permeability shown in Fig. 10a is shown in terms of energy loss $W(f)$ and its components in Fig. 10b. The dynamic loss is here decomposed into the rotational $W_{\mathrm{rot}}(f)$ and the dw generated excess loss $W_{\mathrm{exc}}(f)$ components. $W_{\mathrm{rot}}(f)$ is obtained by introducing $\mu'_{\mathrm{rot}}(f)$ and $\mu''_{\mathrm{rot}}(f)$, as calculated with Eqs. (8) and (9), in Eq. (2) for J_p = 50 mT. The fitting curve applies to the eddy-current-free samples, where we see that beyond 1-2 MHz the measured loss basically coincides with the calculated $W_{\mathrm{rot}}(f)$ fitting curve. The loss in the thicker sample is obtained by adding $W_{\mathrm{cl,eddy}}(f)$, calculated with Eq. (1) to $W_{\mathrm{rot}}(f)$. The excess loss is shown in the same figure to follow a power law dependence on frequency $W_{\mathrm{exc}}(f) \propto f^{\,m}$, with m ranging in the differently treated materials between 0.75 and 0.95. To note that in steel sheets, where the eddy currents provide for efficient shielding of the applied field and faster homogenization of the magnetization process with frequency, it is generally $W_{\mathrm{exc}}(f) \propto f^{\,0.5}$. As previously discussed, we are entitled to apply a generalized formulation of the STL, introducing the spin damping coefficient β_{sd} and neglecting the eddy-current coefficient β_{eddy}. By following the usual procedure for the excess loss analysis,[27] we have

$$W_{\mathrm{exc}}(f, J_{\mathrm{p}}) = 4H_{\mathrm{exc}}J_{\mathrm{pdw}} = 2V_0 n_0 \cdot \left[-1 + \sqrt{1 + \frac{4}{n_0^2 V_0}\beta_{\mathrm{sd}}\frac{S}{<s>}\frac{J_{\mathrm{pdw}}}{J_{\mathrm{s}}^2} f}\right] \cdot J_{\mathrm{pdw}} \, , \tag{11}$$

where the parameters n_0 and V_0 represent, according to the STL, the number of magnetically active magnetic objects (e.g., grains/dw assembly where the threshold field for reversal is overcome) in the limit $f \rightarrow 0$ and V_0, normalized to the dw contribution J_{pdw}, is a loose measure of the coercivity of the material. The analysis of the present results shows that $W_{exc}(f)$ is chiefly influenced by the relative dw contribution J_{pdw}/J_p.

Let us then analyze the $W(f)$ behavior, by assessing response and relative proportions of $W_{rot}(f)$ and $W_{exc}(f)$ as a function of frequency. The representative theoretical predictions of $W_{rot}(f)$ shown in Fig. 11, while justifying the experimentally found merging of all $W(f)$ curves in the MHz range, show that $W_{rot}(f)$ is influenced by doping and temperature only in the relatively narrow frequency interval ~200 kHz - ~ 2 MHz. It is also observed that optimal doping weakens the dependence on temperature of $W_{rot}(f)$, but the effect of shifting the function $g(H_{k,eff})$ towards lower $H_{k,eff}$ values is conducive to somewhat larger $W_{rot}(f)$ values at lower frequencies. The representative loss decomposition shown in Fig. 10b puts in evidence that W_h, $W_{exc}(f)$ and $W_{rot}(f)$ are prevalent on specific frequency intervals. $W_{exc}(f)$, in particular, is generally important between 100 kHz and 1 MHz, as put in evidence in Fig. 12. This figure, providing an illustrative comparison among the loss components up to a few MHz. makes clear that, similar to the common case of steel sheets, W_h and $W_{exc}(f)$ display correlated behaviors, both decreasing with increasing temperature and showing, consistent with the $<K_{eff}>$ behavior (Fig. 7), larger spread of values with T in the highly doped ferrites. A reverse trend with T is exhibited by the $W_{rot}(f)$ curves, whose separation, however, is coherently reduced in the CoO = 4000 ppm samples. $W_{exc}(f)$ is in any case affordable by means of Eq. (11), as applied to the experimental $W_{exc}(f)$ using to the standard procedure envisaged by the STL.[27] An example of application of Eq. (11) is given in Fig. 13, where the decrease of $W_{exc}(f)$ at given J_p upon doping turns out to be mainly justified in terms of reduced dw contribution J_{pdw}.

V. CONCLUSION

The effect of CoO-doping (0 – 6000 ppm) on the temperature dependence of loss and permeability in Mn-Zn ferrites has been physically assessed by identification and separation of the dw and rotational processes, determination of the average effective magnetic anisotropy constant as a function of doping and temperature, and analysis of the energy loss behavior up to 1 GHz. The investigation covers in this way the whole frequency range where the magnetic response of the material, characterized by distributed ferromagnetic resonance, can be appreciated. The magnetic anisotropy $<K_{eff}>$, obtained through the identification of the dc rotational permeability, exhibits a monotonical decrease upon increasing the temperature, from a maximum value of 155 J/m^3 at T = -20 °C in the highly doped ferrite (CoO = 6000 ppm) to a minimum value around 13 J/m^3 in all samples at T = 130 °C. The highest stability of $<K_{eff}>$ versus T is obtained in the CoO = 3000 ppm doped ferrites, where it attains a maximum value of 43 J/m^3 at T = -20 °C. Based on these findings, we justify the observed dependence of the quasi-static energy loss W_h on temperature and CoO content by a conventional formulation involving $<K_{eff}>$ and the found proportion of the dw contribution J_{pdw} to the peak polarization value J_p.

The broadband dynamic behavior of the material, characterized by the relaxation of dw motion and the resonant response of the rotational processes, with the former vanishing on entering the MHz range, is described by separating first any possible eddy current effect (classical eddy current losses) and formulating then general expressions for the real and imaginary permeability components, starting from the solutions of the Landau-Lifshitz equation and making the required averaging over amplitude and orientation distributions of the local magnetic anisotropies. The so-calculated spin damping loss W_{rot}, shown to excellently fit the high-frequency experimental results, appears to appreciably depend on

doping and temperature only on a relatively restricted frequency range, from a few hundred kHz to a few MHz. The dynamic loss contribution by dw displacements W_{exc} is determined and found to follow a power law dependence on frequency, in accordance with the STL based theoretical formulation. For any degree of doping, W_h, W_{exc}, and W_{rot} are prevalent on contiguous frequency bands, as illustrated in the loss decomposition map of Fig. 14, whose position and width versus temperature is in a direct relationship with the temperature dependence of the calculated anisotropy $<K_{eff}>$.

SUPPLEMENTARY MATERIAL

See supplementary material for further illustrative data concerning the broadband loss and permeability behaviors of the Mn-Zn ferrites for different levels of CoO doping, their temperature dependence, and their assessment by the generalized STL approach.

ACKNOWLEDGMENT

This work was performed in the context of the Agreement of Scientific and Technological Cooperation between the Istituto Nazionale di Ricerca Metrologica (INRIM) and The Centre for Research and Technology Hellas (CERTH) regarding the study of soft ferrites.

The authors wish to thank Dr. A. Merlone and Dr. C. Musacchio of INRIM for assistance in the low-temperature measurements.

REFERENCES

[1]H. Shokrollahi and K. Janghorban, "Influence of additives on the magnetic properties, microstructure and densification of Mn-Zn soft ferrites," Mater. Sci. Eng. B 141, 91–107 (2007), doi: 10.1016/j.mseb.2007.06.005.
[2]A. Znidarsic, M. Limpel, and M. Drofenik, "Effect of dopants on the magnetic properties of MnZn ferrites for high frequency power supplies," IEEE Trans. Magn. 31, 950–953 (1995), doi: 10.1109/20.364767.
[3]H. Pascard, "Basic concepts for high permeability in soft ferrites," J. Phys IV (France) 8-Pr2, 377-384 (1998), doi: 10.1051/jp4:1998288.
[4]V.T. Zaspalis, and E. Eleftheriou, "The effect of TiO_2 on the magnetic power losses and electrical resistivity of polycrystalline MnZn ferrites," J. Phys. D 38, 2156-2161 (2005), doi: 10.1088/0022-3727/38/13/012
[5]A. Gonchar, S. Katynkina, L. Letyuk, and I. Ryabov, "The influence of microstructure parameters on the magnetic losses in soft magnetic ferrites for television engineering," J. Magn. Magn. Mater. 215-216, 224-226 (2000), doi: 10.1016/S0304-8853(00)00122-0.
[6]L. Li, Z. Lan , Z. Yu, and K. Sun, "Influence of Fe_2O_3 stoichiometry on initial permeability and temperature dependence of core loss in MnZn ferrites," IEEE Trans. Magn. 44, 13–16 (2008), doi: 10.1109/TMAG.2007.910232.
[7]V. Zaspalis, V. Tsakaloudi, E. Papazoglou, M. Kolenbrander, R. Guenther, and P. van der Valk, "Development of a new MnZn ferrite soft magnetic material for high temperature power applications," J. Electroceramics 13, 585-591 (2004), doi: 10.1007/s10832-004-5162-3.
[8]J. Hanuszkiewicz, D. Holz, E. Eleftheriou, and V.T. Zaspalis, "Materials processing issues influencing the frequency stability of the initial magnetic permeability of MnZn ferrites," J. Appl. Phys. 103, 103907 (2008), doi: 10.1063/1.2932062.
[9]A. Fujita and S. Gotoh, "Temperature dependence of core loss in Co-substituted MnZn ferrites," J. Appl. Phys. 93, 7477-7479 (2003), doi: 10.1063/1.1557952.
[10]S. Wang, Y. Chiang, Y. Hsu and C. Chen, "Effects of additives on the loss characteristics of Mn-Zn ferrite," J. Magn. Magn. Mater. 365, 119-125 (2014), doi: 10.1016/j.jmmm.2014.04.043.
[11]V. Tsakaloudi, G. Kogias, and V.T. Zaspalis, "A new power MnZn ferrite for broad temperature range applications," J. Magn. Magn. Mater. 365, 119-125 (2014), doi: 10.1016/j.jmmm.2014.04.043.
[12]G. Herzer, "Nanocrystalline soft magnetic alloys," in *Handbook of Magnetic Materials*, vol. 10, edited by K.H.J. Buschow (Elsevier Science, Amsterdam, 1997), pp. 415-462, doi: 10.1016/S1567-2719(97)10007-5.

[13]A.D. Giles and F.F. Westendorf, "The effect of cobalt substitutions on some properties of manganese zinc ferrites," J. Phys. D: Appl. Phys. 9, 2117-2122 (1976), doi: 10.1088/0022-3727/9/14/020.
[14]L. Li, Z. Lan, Z. Yu, K. Sun, and Z. Xu, "Effects of Co-substitution on wide temperature ranging characteristic of electromagnetic properties in MnZn ferrites," J. Alloys Comp. 476, 755-759 (2009), doi: 10.1016/j.jallcom.2008.09.101.
[15]K. Mori, K. Yasuhara, I. Nakahata, and K. Nishikawa, "High temperature stability of Co-doped MnZn ferrites for automobiles," J. Jpn. Soc. Powder Powder Metall. 61-S1, 224-226 (2014), doi: 10.2497/jjspm.61.S224.
[16]C. Beatrice, V. Tsakaloudi, S. Dobák, V. Zaspalis, and F. Fiorillo, "Magnetic losses versus sintering treatment in Mn-Zn ferrites," J. Magn. Magn. Mater. 429, 129-137 (2017), doi: 10.1016/j.jmmm.2016.12.121.
[17]E. Ferrara, F. Fiorillo, C. Beatrice, S. Dobák, C. Ragusa, A. Magni, and C. Appino, "Characterization and assessment of the wideband magnetic properties of nanocrystalline alloys and soft ferrites," J. Mater. Res. 33, 2120-2137 (2018), doi: 10.1557/jmr.2018.275.
[18]D. Stoppels, "Developments in soft magnetic power ferrites," J. Magn. Magn. Mater. 160, 323-328 (1996), doi: 10.1016/0304-8853(96)00216-8.
[19]K. Sun, Z. Lan, Z. Yu, L. Li, X. Jiang, and H. Ji, "Temperature dependence of core losses at high frequencies for MnZn ferrites," Physica B. 405, 1018-1021 (2010), doi: 10.1016/j.physb.2009.10.047.
[20]M. LoBue, F. Mazaleyrat, and V. Loyau, "Study of magnetic losses in Mn-Zn ferrites under biased and asymmetric excitation waveforms," IEEE Trans. Magn. 46, 451-454 (2010), doi: 10.1109/TMAG.2009.2031471.
[21]O. de la Barrière, C. Appino, F. Fiorillo, C. Ragusa, M. Lecrivain, L. Rocchino, H. Ben Ahmed, M. Gabsi, F. Mazaleyrat, and M. Lo Bue, "Characterization and prediction of magnetic losses in soft magnetic composites under distorted induction waveforms," IEEE Trans. Magn. 49, 1318-1326 (2013), doi: 10.1109/TMAG.2012.2218614.
[22]F. V. Loyau, G.-Y. Wang, M. LoBue, and F. Mazaleyrat, "An analysis of Mn-Zn ferrite microstructure by impedance spectroscopy, scanning transmission electron microscopy and energy dispersion spectrometry characterizations," J. Appl. Phys., 111, 053928 (2012), doi: 10.1063/1.3693544.
[23]F. Fiorillo, C. Beatrice, O. Bottauscio, and E. Carmi, "Eddy current losses in Mn-Zn ferrites," IEEE Trans. Magn. 50 6300109 (2014), doi: 10.1109/TMAG.2013.2279878.
[24]C. Beatrice, S. Dobák, V. Tsakaloudi, C. Ragusa, F. Fiorillo, L. Martino, and V. Zaspalis, "Magnetic loss, permeability, and anisotropy compensation in CoO-doped Mn-Zn ferrites," AIP Adv. 8, 047803 (2018), doi: 10.1063/1.4993718.
[25]F. Fiorillo and C. Beatrice, "A comprehensive approach to broadband characterization of soft ferrites," Int. J. Appl. Electromagn. Mech. 48, pp. 283–294 (2015), doi: 10.3233/JAE-152000.
[26]J.F. Dillon, Jr. and H.E. Earl, Jr., "Domain wall motion and ferromagnetic resonance in a manganese ferrite," J. Appl. Phys. 30, pp. 202-213 (1959), doi: 10.1063/1.1735134.
[27] G. Bertotti, *Hysteresis in Magnetism* (Academic Press, San Diego, CA, USA, 1998), p. 411.

FIGURE CAPTIONS

Fig. 1. Energy loss $W(f)$ versus frequency at different temperatures in CoO = 3000 ppm doped Mn-Zn ferrite ring samples before and after thickness reduction from d = 4.97 mm to d = 1.30 mm. The measurements have been performed by a fluxmetric method up to about 2 MHz (symbols) and by means of a Vector Network Analyzer (VNA) at higher frequencies (lines). The eddy current loss $W_{cl,eddy}$ plays a role beyond a few MHz in the thicker sample. The solid and open large symbols provide the high-frequency values of $W_{cl,eddy}$, calculated with Eq. (1), on the thick and thin samples, respectively. Eddy-current-free loss can be assumed for the d = 1.30 mm thick sample. The inset shows how the VNA and fluxmetrically measured $W(f)$ curves overlap, for J_p = 2 mT, over a large frequency interval (the dashed line refers to the thin sample).

Fig. 2. Frequency dependence (up to f = 20 MHz) of the real $\rho'(f)$ (a) and imaginary - $\rho''(f)$ (b) resistivity components of a CoO-doped Mn-Zn ferrite. The significant decrease of ρ'_{DC} with temperature reflects increased conductivity of the grain boundary layers. The minor effect on $\rho'(f)$ at high frequencies points to a weak change of the intragrain conductivity with temperature.

Fig. 3. Initial DC permeability μ_i measured from –20 °C to 130 °C in CoO-doped Mn-Zn ring samples. Restrained $\mu_i(T)$ evolution is achieved for CoO = 3000-4000 ppm.

Fig. 4. Same as Fig. 3 for the quasi-static hysteresis loss W_h at J_p = 50 mT.

Fig. 5. The energy loss dependence on temperature is smoothed out, for all CoO concentrations, with the increase of the magnetizing frequency.

Fig. 6. Example of the behavior of the broadband real permeability $\mu'(f)$ in a CoO = 6000 ppm ring sample at 85 °C. The real permeability component measured fluxmetrically at J_p = 10 mT and J_p = 50 mT up to a few MHz (symbols) overlaps with the same quantity measured by the 10 mW transmission line method and VNA (solid line) in the upper frequency range. The rotational $\mu'_{rot}(f)$ and dw $\mu'_{dw}(f)$ components, separately identified, exhibit resonant and relaxation character, respectively. $\mu'_{rot}(f)$ is theoretically predicted (dashed line) through the Landau-Lifshitz equation.

Fig. 7. Effective average anisotropy constant $\langle K_{eff} \rangle$ as a function of temperature and CoO doping.

Fig. 8. Examples of the quasi-static energy loss W_h dependence on CoO content at two temperatures and different J_p values. The dashed line are predicted by Eq. (5).

Fig. 9. The deep minimum of W_h observed for CoO = 3000 – 4000 ppm at room temperature and below, evolves toward slow decrease with CoO on approaching and overcoming T = 100 °C. This behavior becomes predictable by use of Eq. (5).

Fig. 10. a) Broadband permeability of the CoO = 3000 ppm Mn-Zn ferrite (symbols) and its rotational components ($\mu'_{rot}(f)$ and $\mu''_{rot}(f)$, continuous lines). The dashed fitting lines are calculated through Eqs. (8) and (9). b) Corresponding behavior of the energy loss and its components. W_h is obtained as the extrapolated value of $W(f)$ for $f \rightarrow 0$. $W_{rot}(f)$ is calculated with Eq. (11). $W_{exc}(f)$ exhibits a power law dependence on f and drops rapidly on approaching the MHz region, following the relaxation of the dw displacements. $W_{rot}(f)$ is negligible with respect to $W_{exc}(f)$ and W_h at frequencies lower than a few hundred kHz.

Fig. 11. Rotational loss $W_{rot}(f)$ calculated for the undoped and the CoO = 3000 ppm doped ferrites at different temperatures. The rotational losses are influenced by doping and temperature only between a few hundred kHz and 1-2 MHz, a region where, for a same temperature, they are higher in the doped material.

Fig. 12. The loss components in the Mn-Zn ferrites are compared at different temperatures for two levels of CoO doping. W_h, $W_{exc}(f)$, and $W_{rot}(f)$ are prevalent at low, intermediate, and high frequencies, respectively. W_h and $W_{exc}(f)$ follow a similar decreasing trend with increasing T, an effect largely magnified in the CoO = 6000 ppm doped ferrite. A reverse trend is displayed by $W_{rot}(f)$, because of concurrent widening of the ferromagnetic resonance spectrum toward low frequencies.

Fig. 13. Comparison of excess and hysteresis loss in undoped and optimally CoO-doped Mn-Zn ferrites at room temperature. The dashed fitting lines have been obtained applying Eq. (11), according to the standard approach of the Statistical Theory of Losses and taking into account the fractional contribution by the dw displacements J_{pdw}/J_p to the full magnetization reversal.

Fig. 14. Loss decomposition map in CoO-doped Mn-Zn ferrites at two temperatures. The lines mark the passage between prevalent loss components (see Fig. 12). The CoO - f shaded areas at intermediate frequencies identify excess loss W_{exc} larger than both W_h and W_{rot}. To remark the substantial stability of the loss decomposition, on passing from T = 23 °C to T = 85 °C, for CoO = 3000 – 4000 ppm, in contrast with the behavior for CoO = 0 and 6000 ppm. It relates to a corresponding behavior of the anisotropy $\langle K_{eff} \rangle$ (Fig. 7).

Journal of Applied Physics

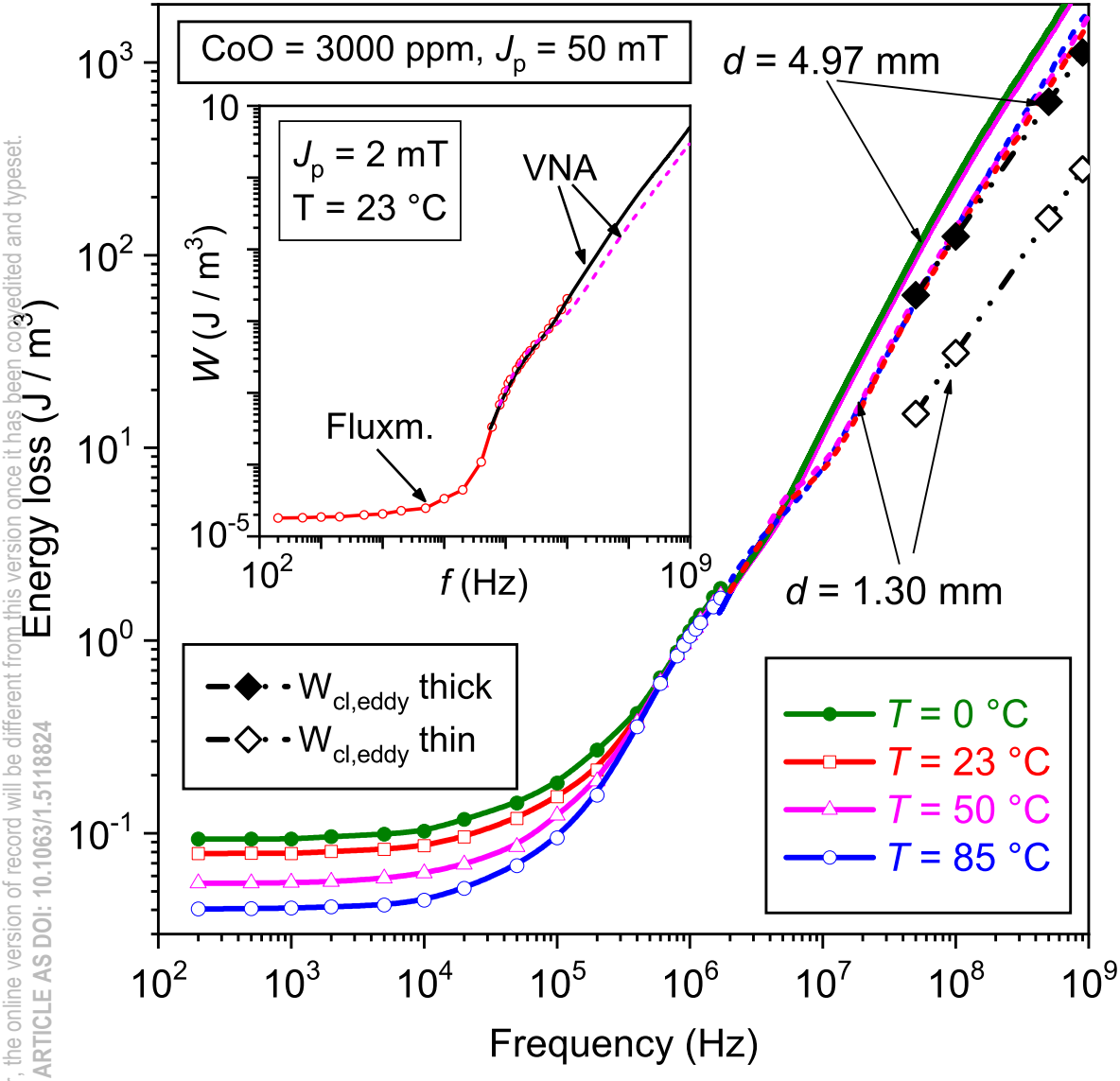

AIP Publishing

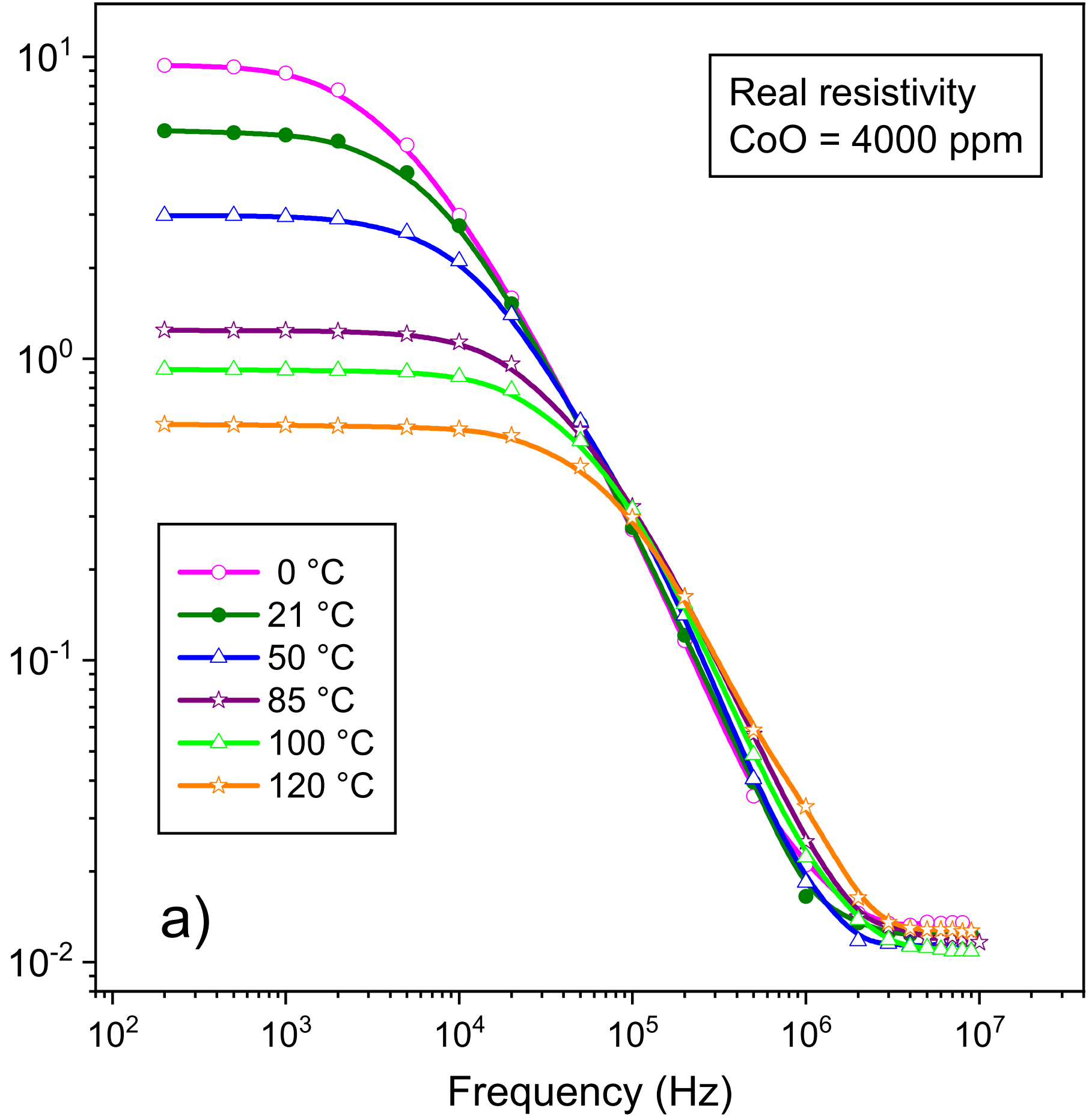

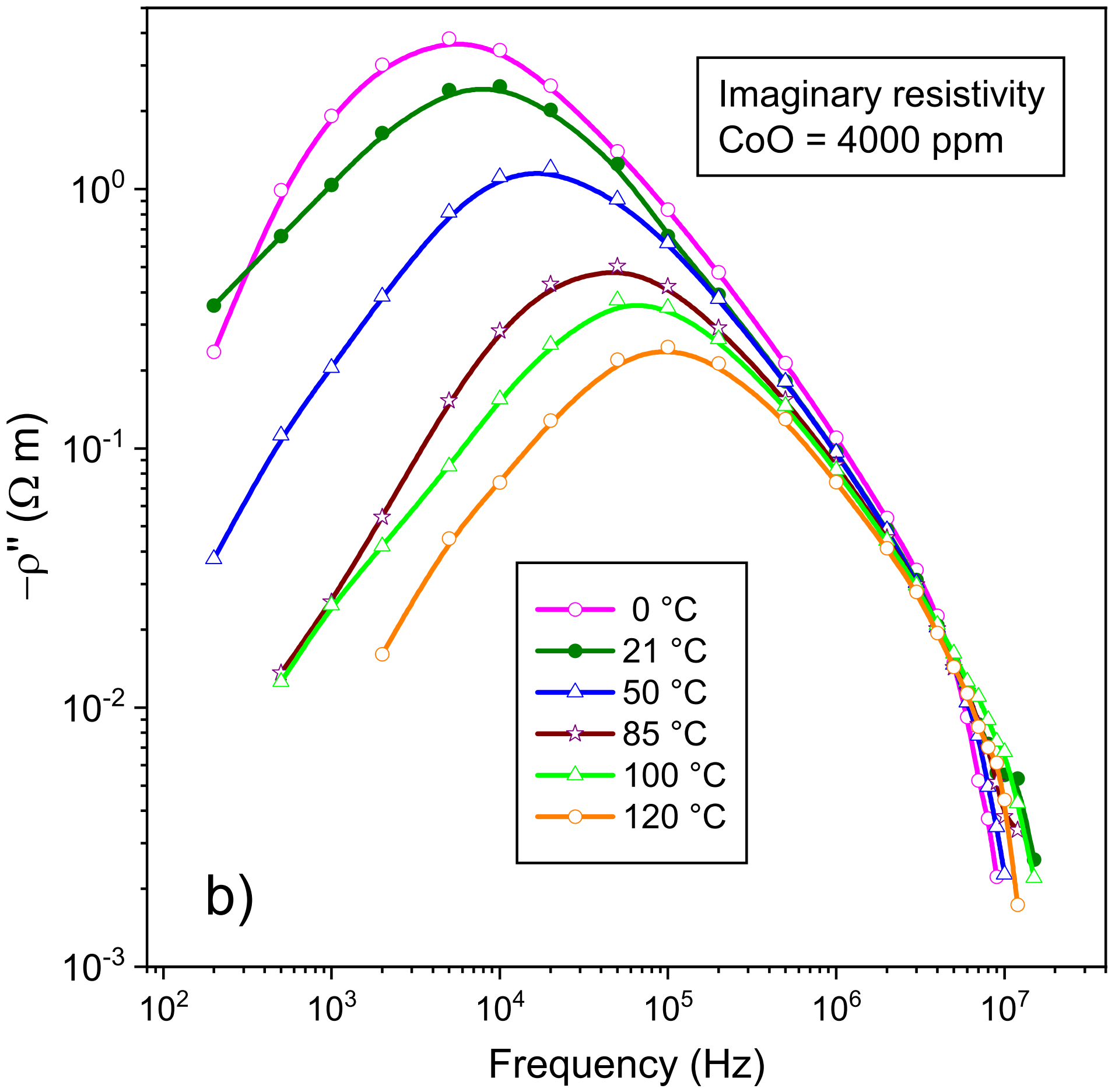

Journal of Applied Physics

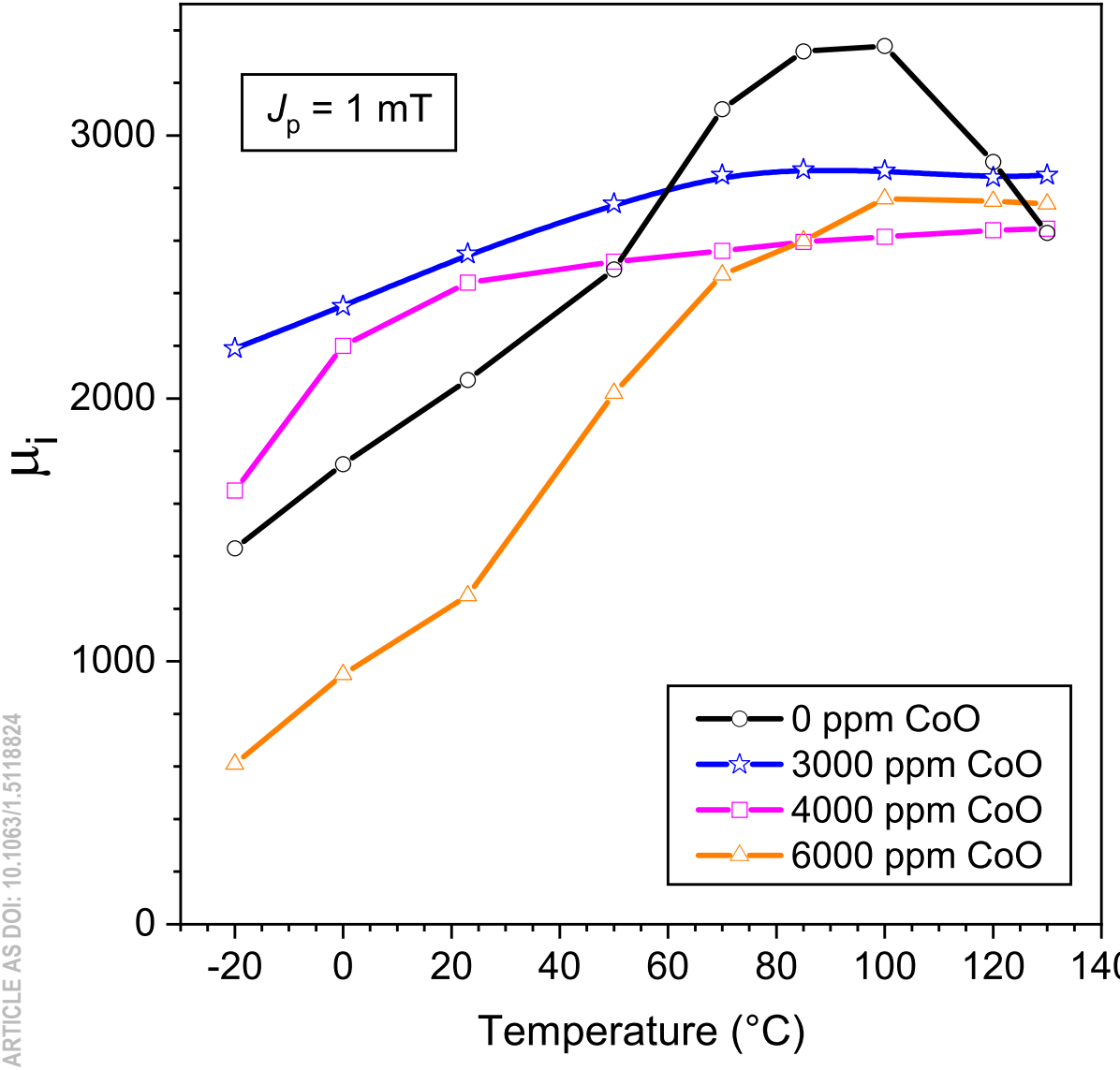

Journal of Applied Physics

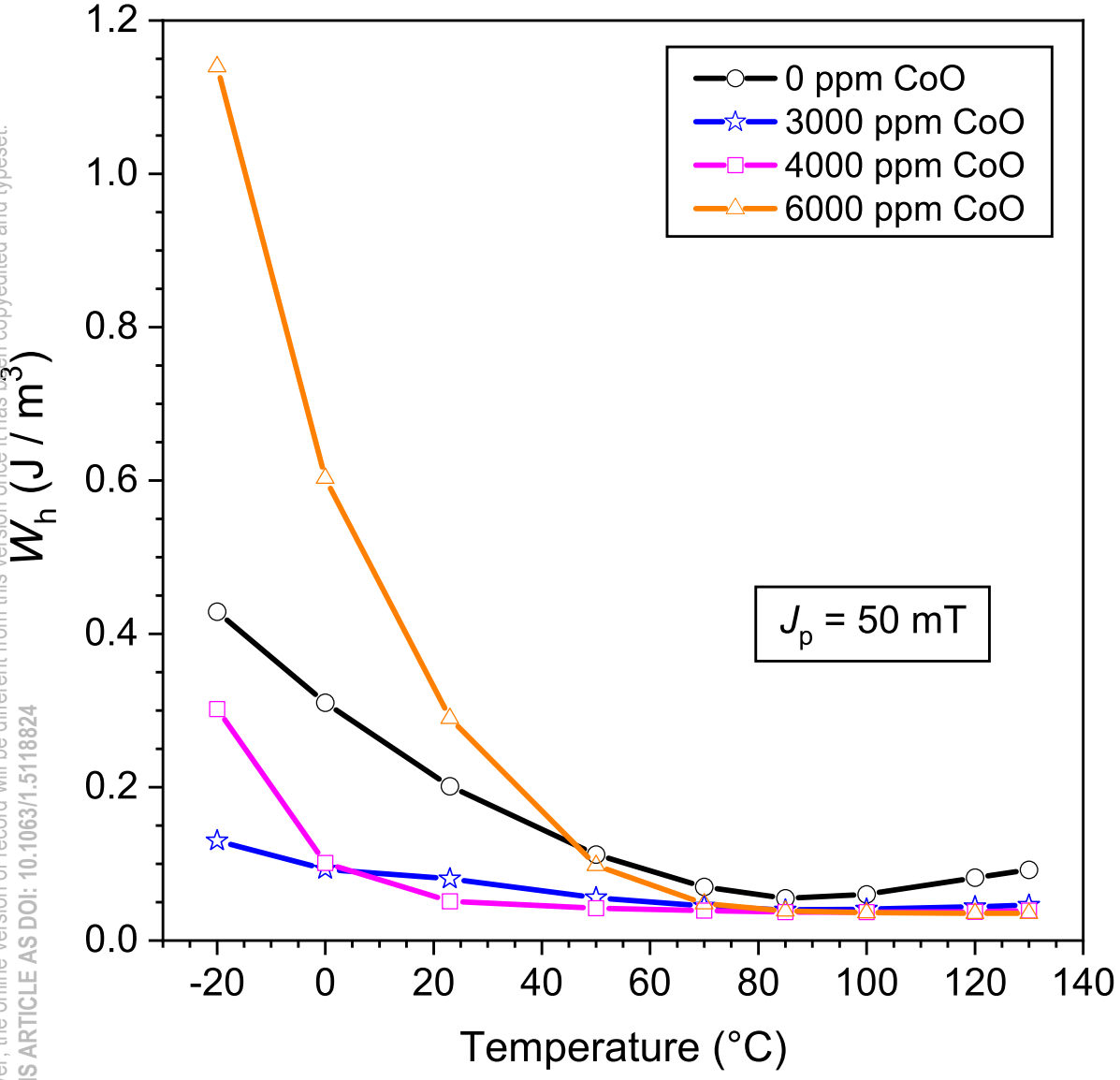

Journal of Applied Physics

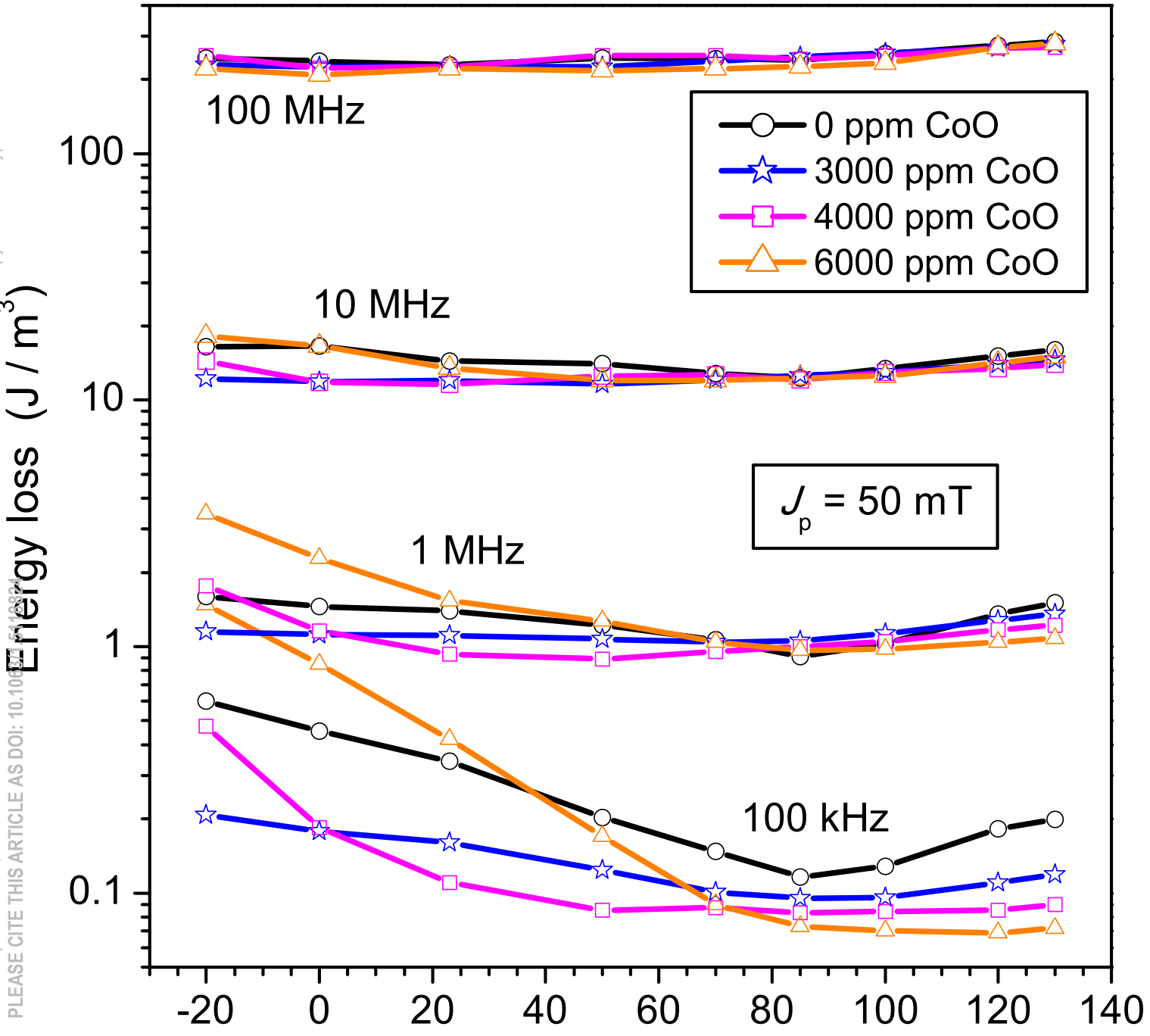

AIP Publishing

Journal of Applied Physics

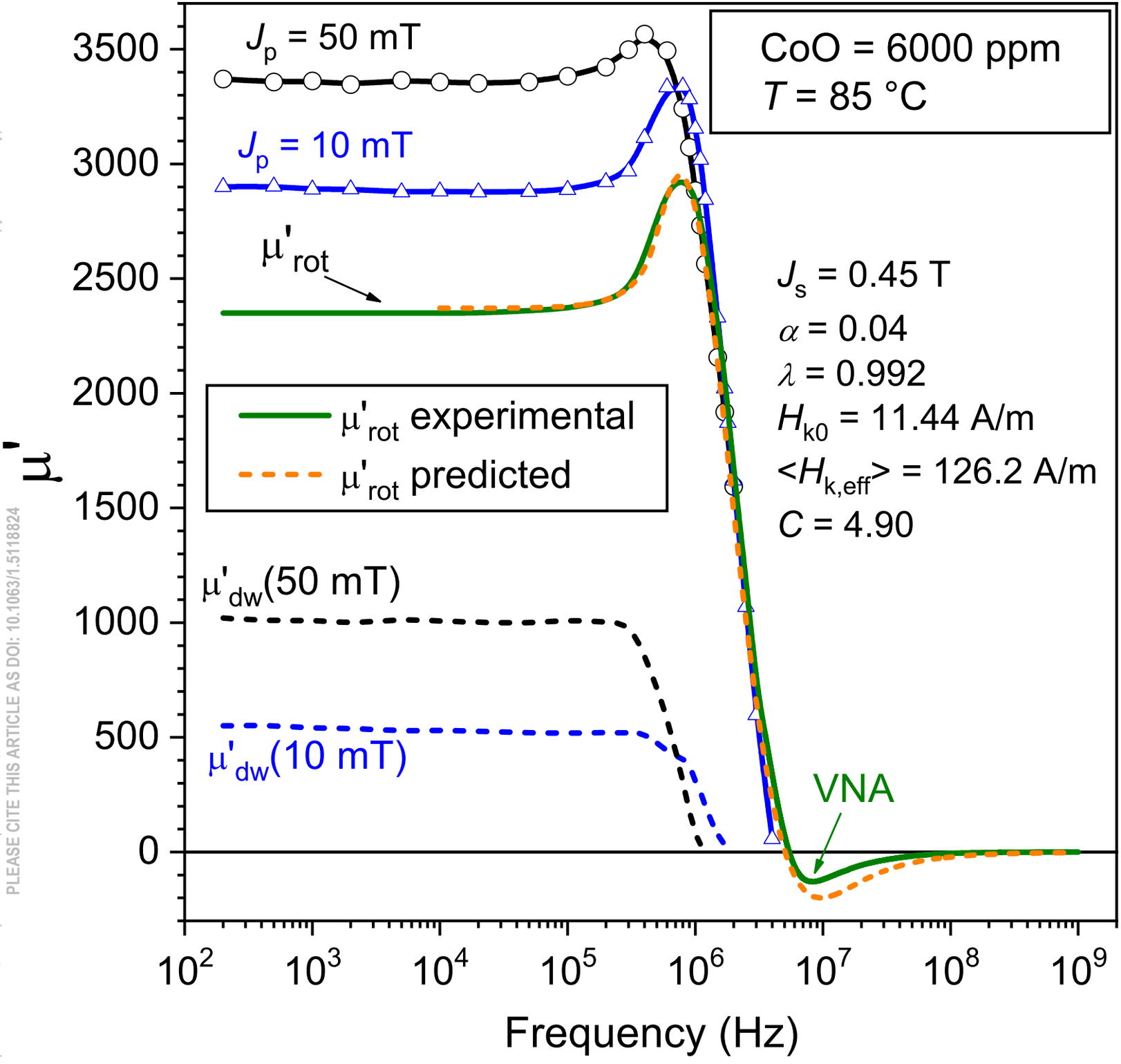

AIP Publishing

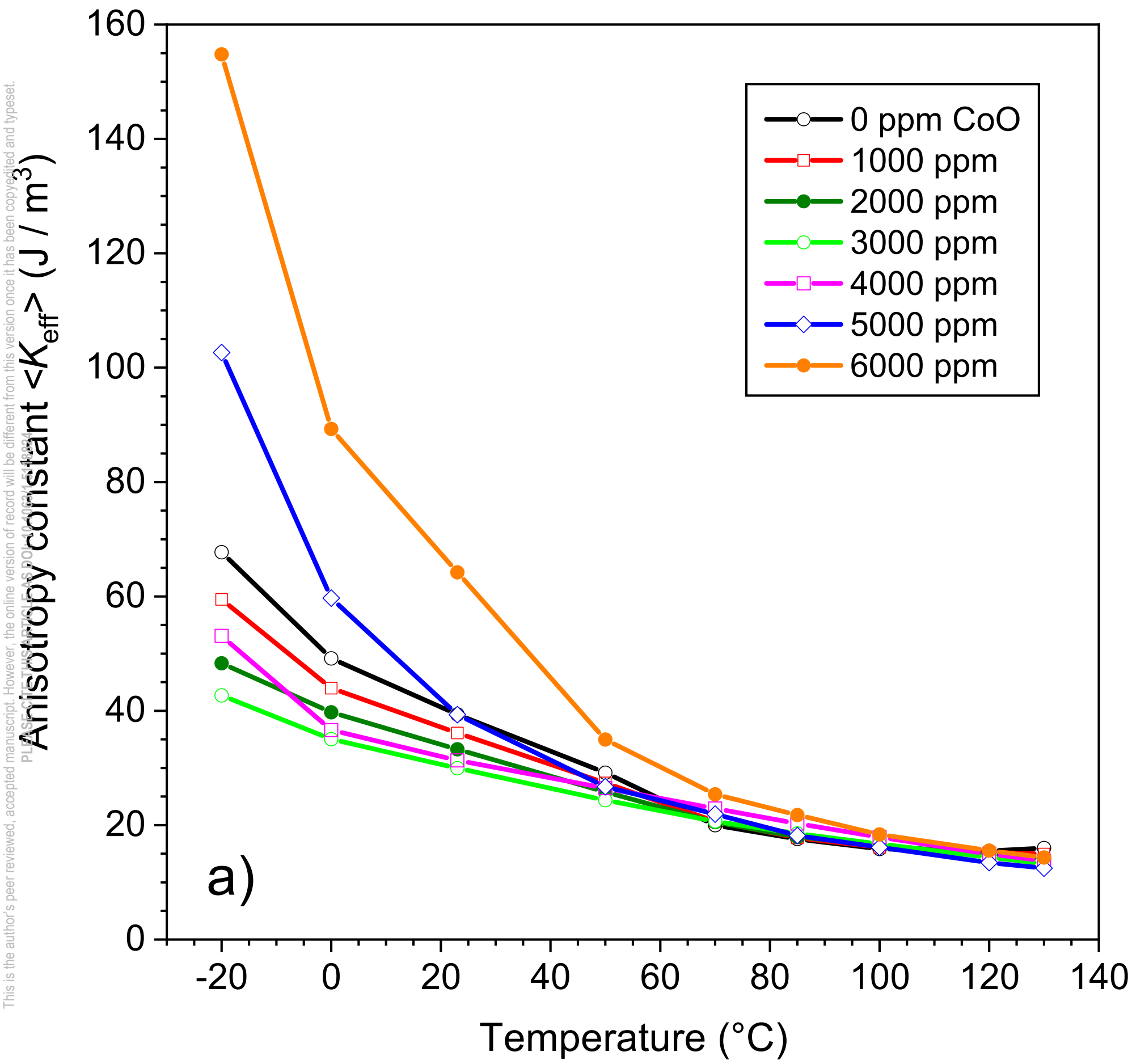

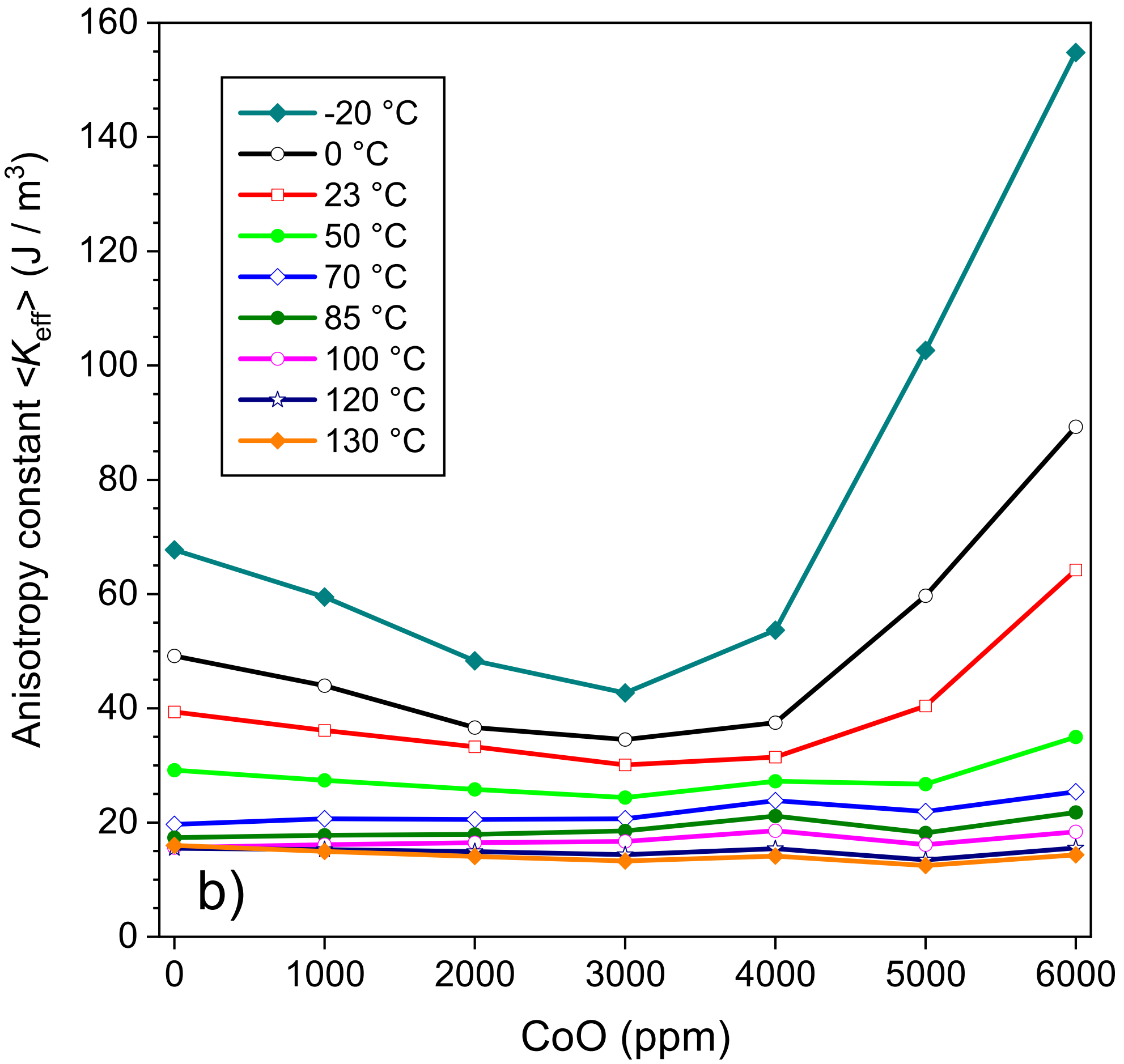

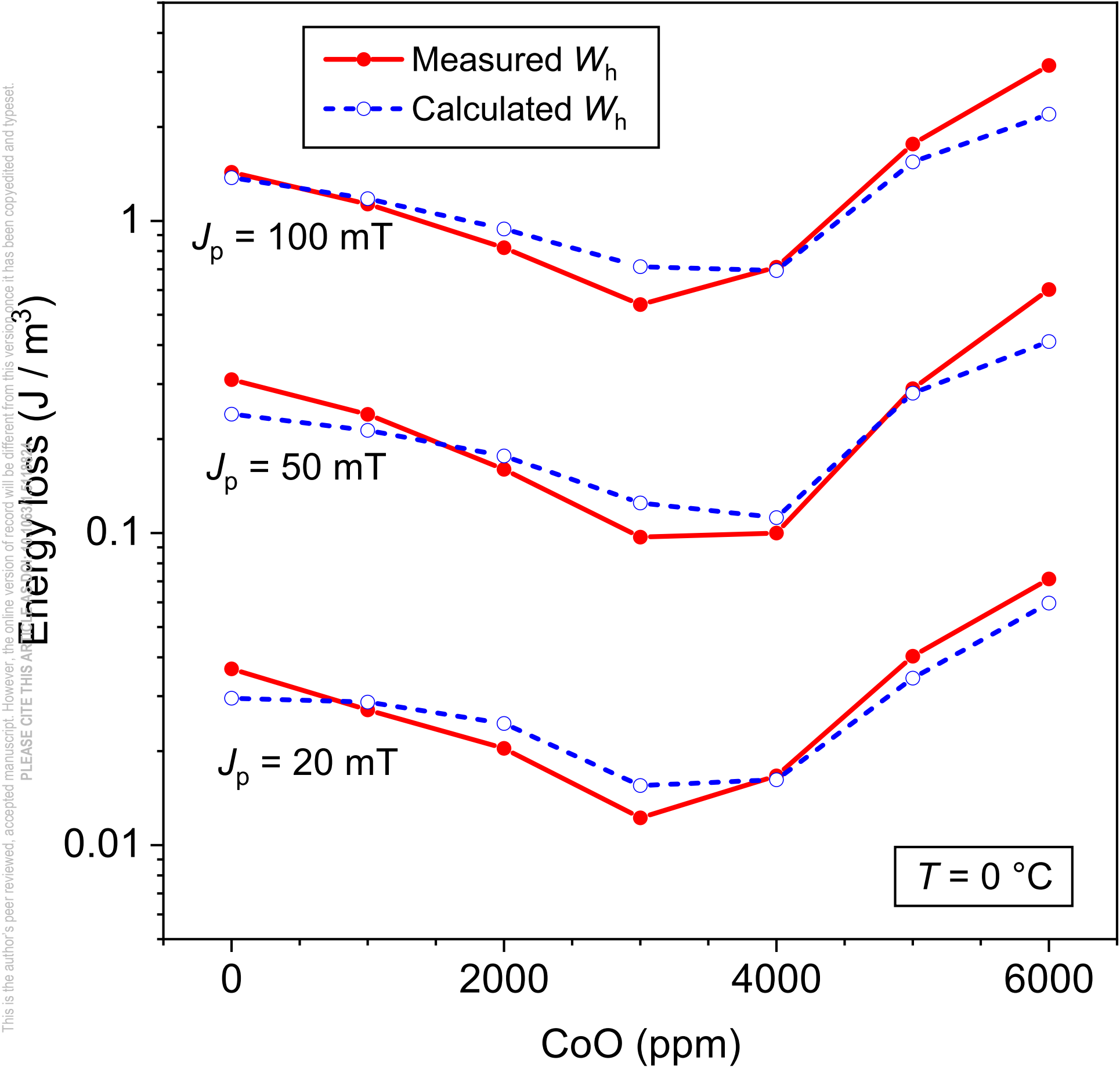

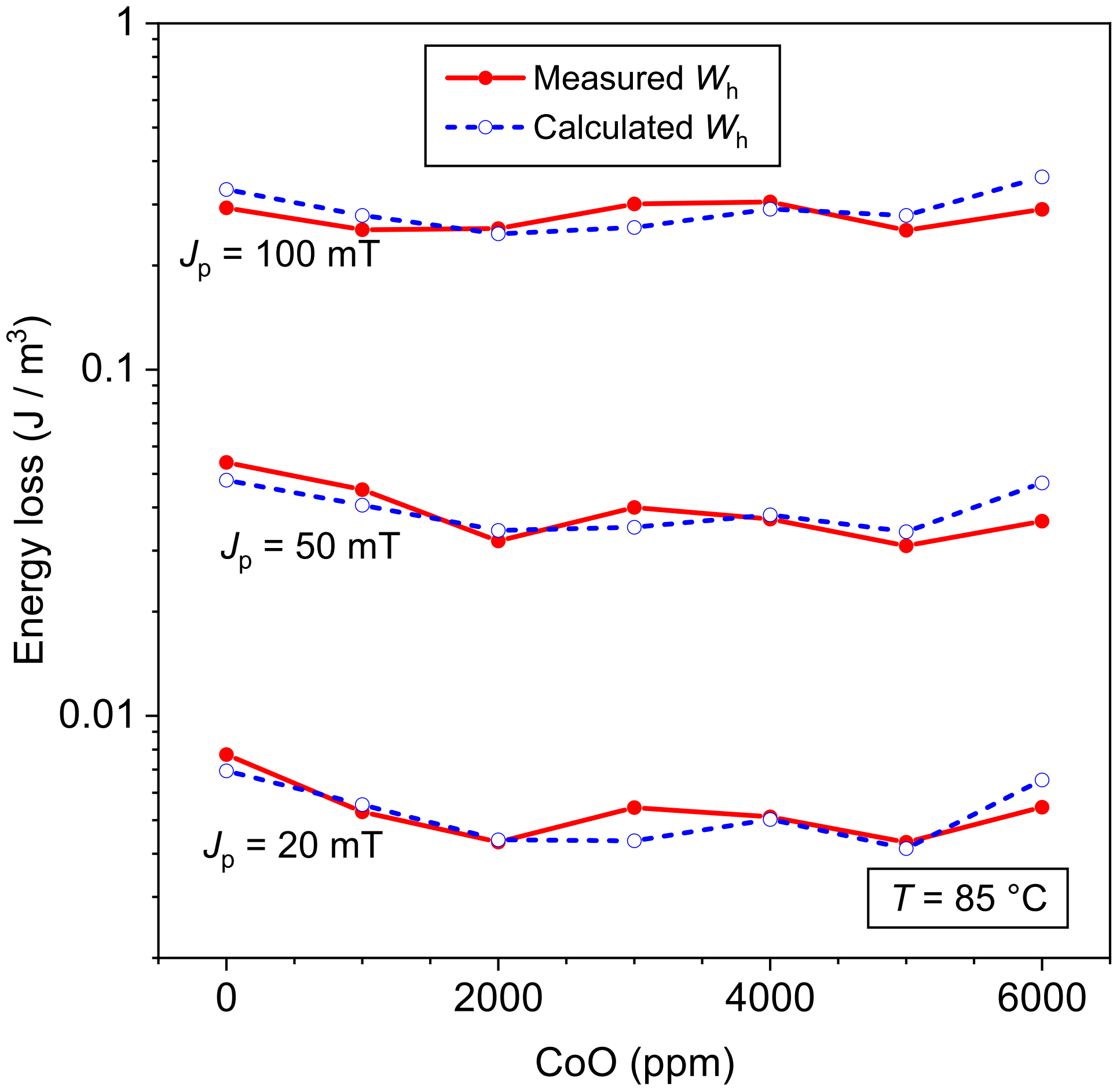

Journal of Applied Physics

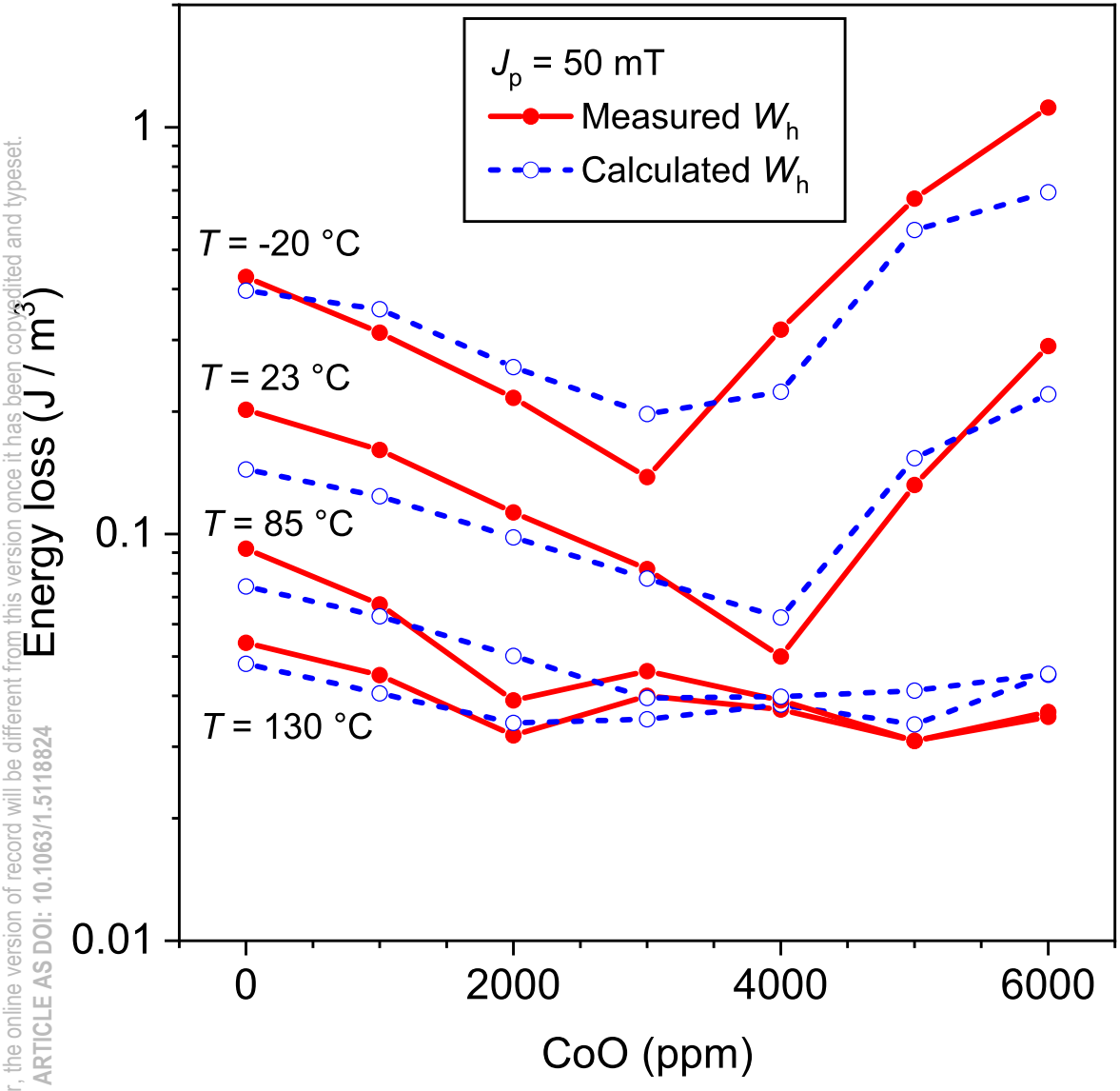

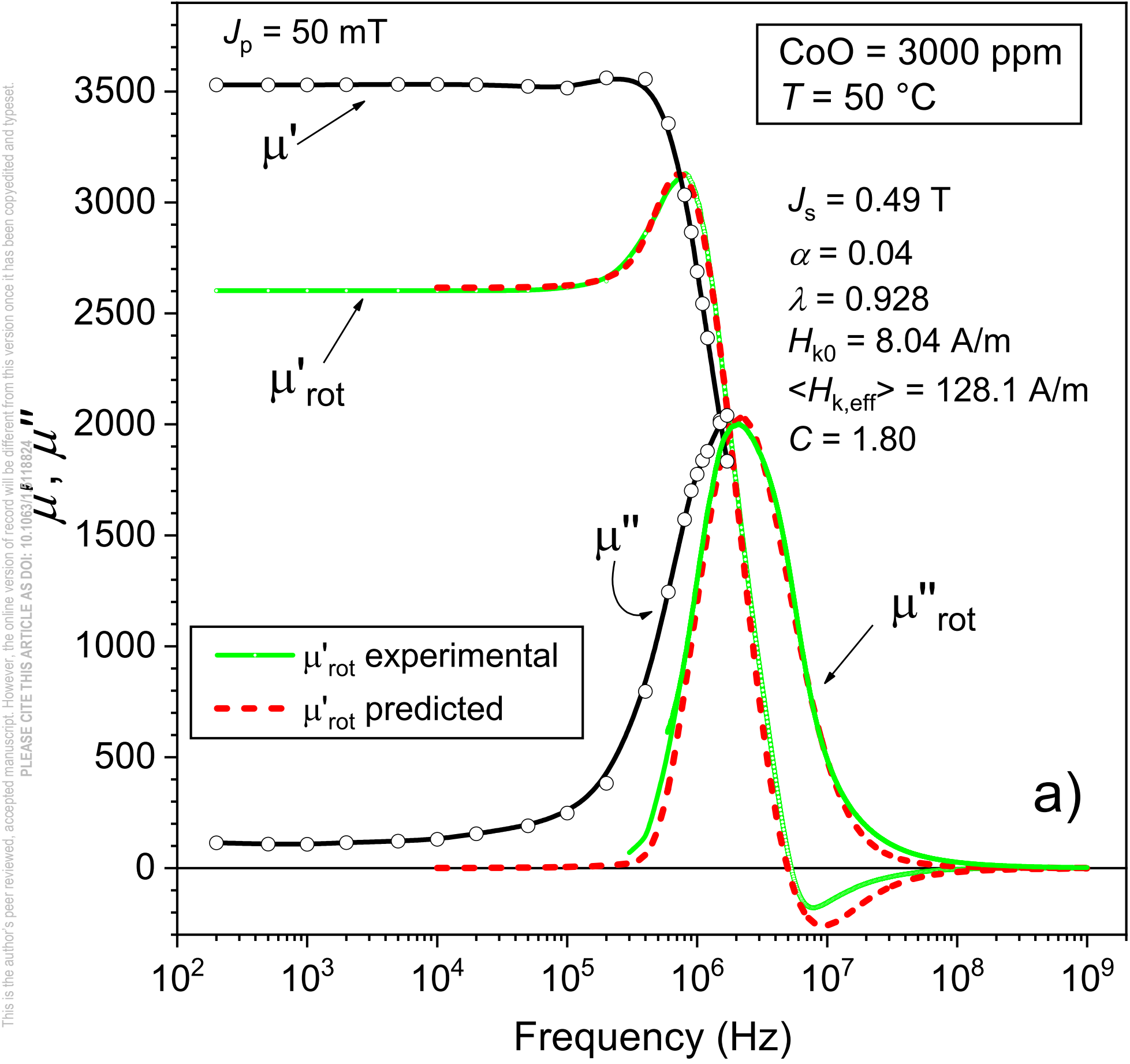

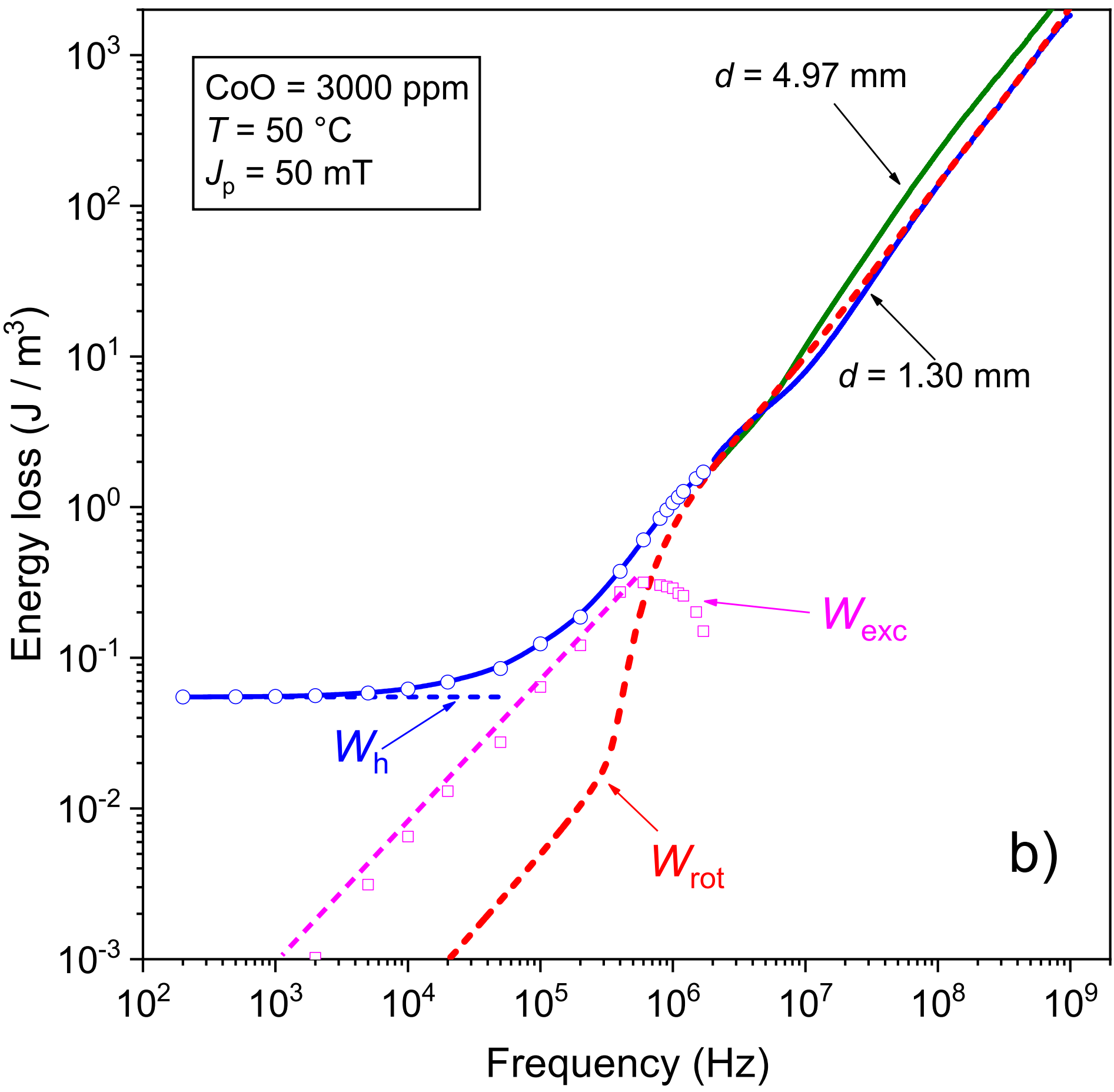

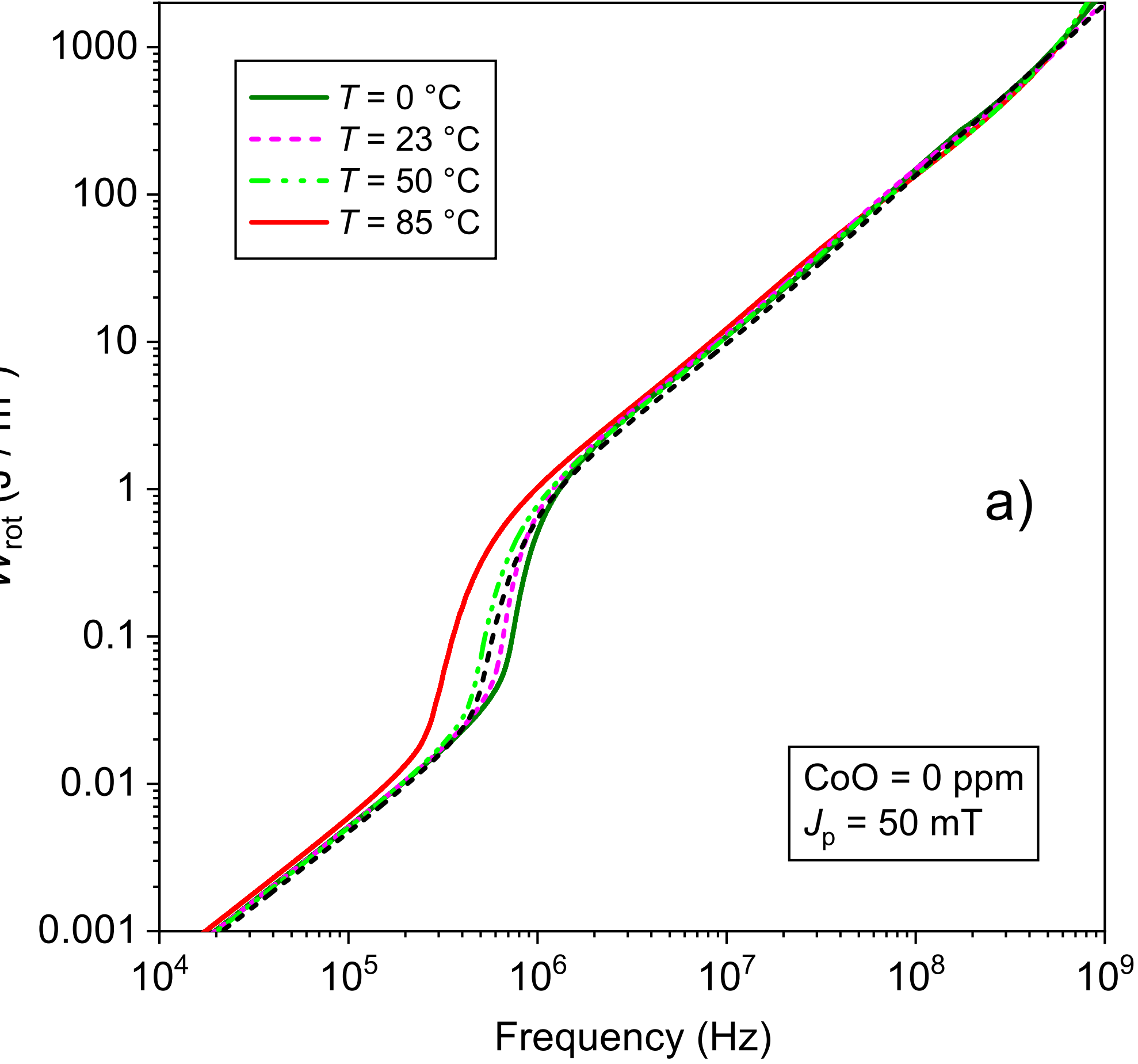

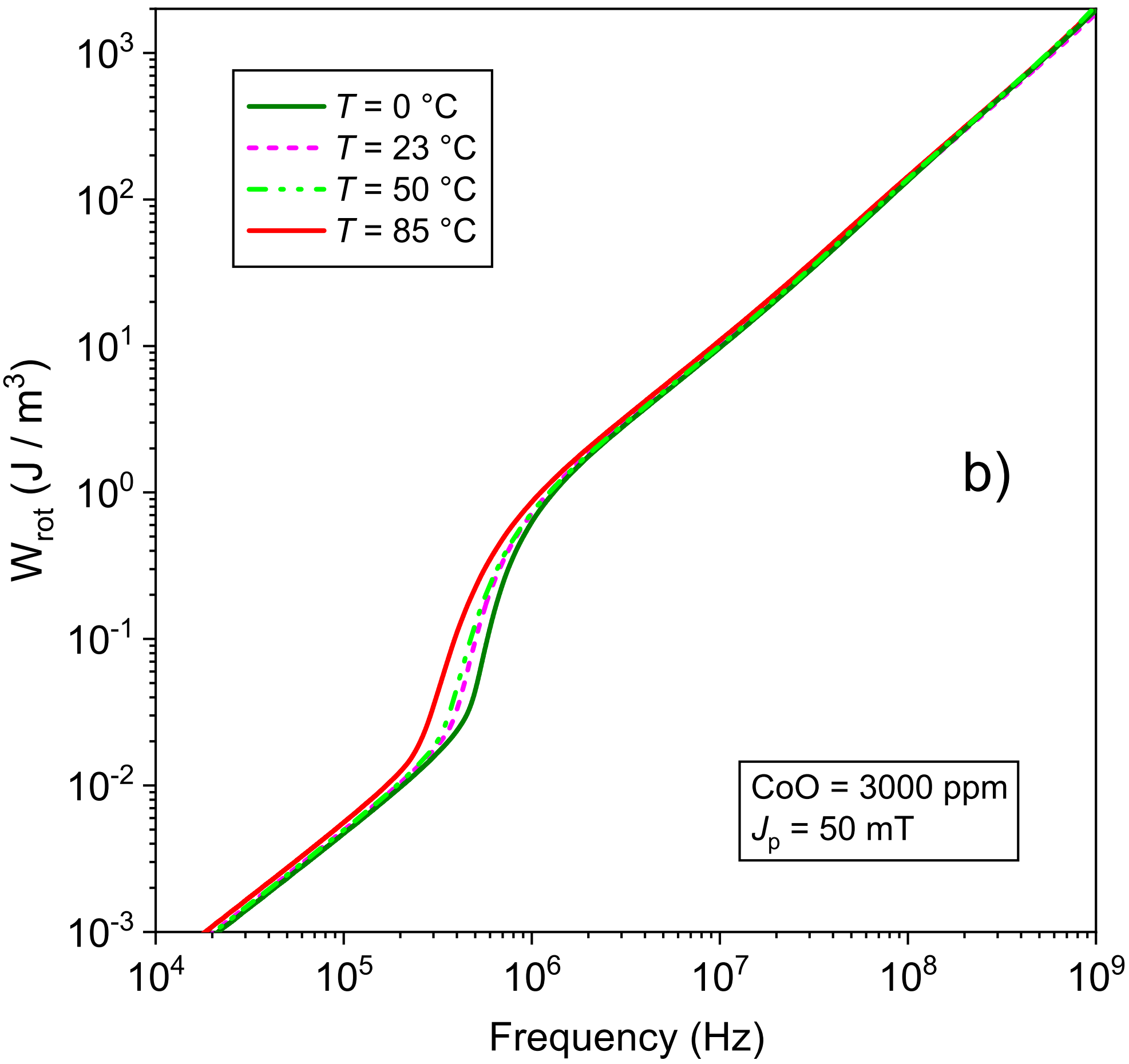

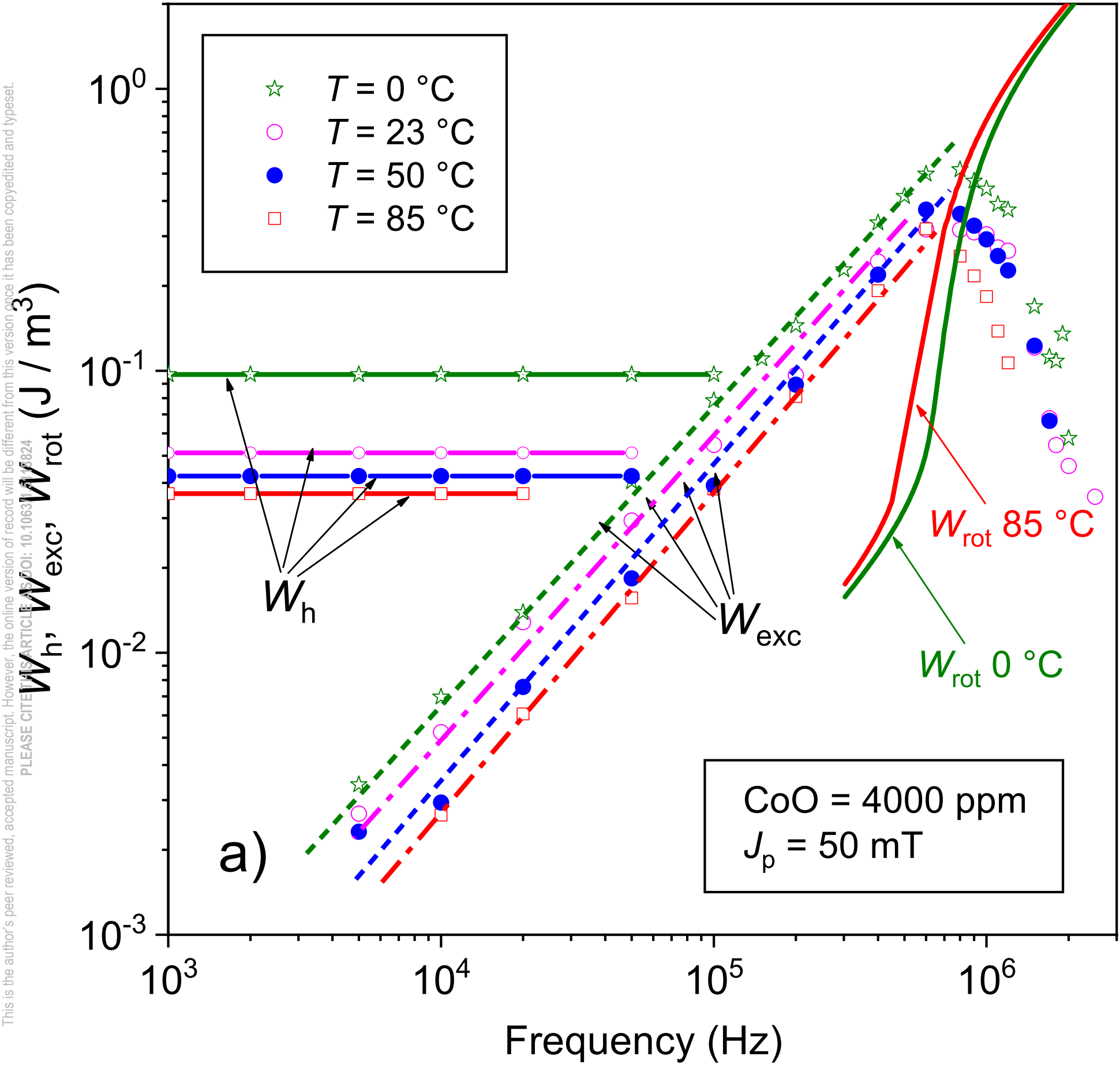

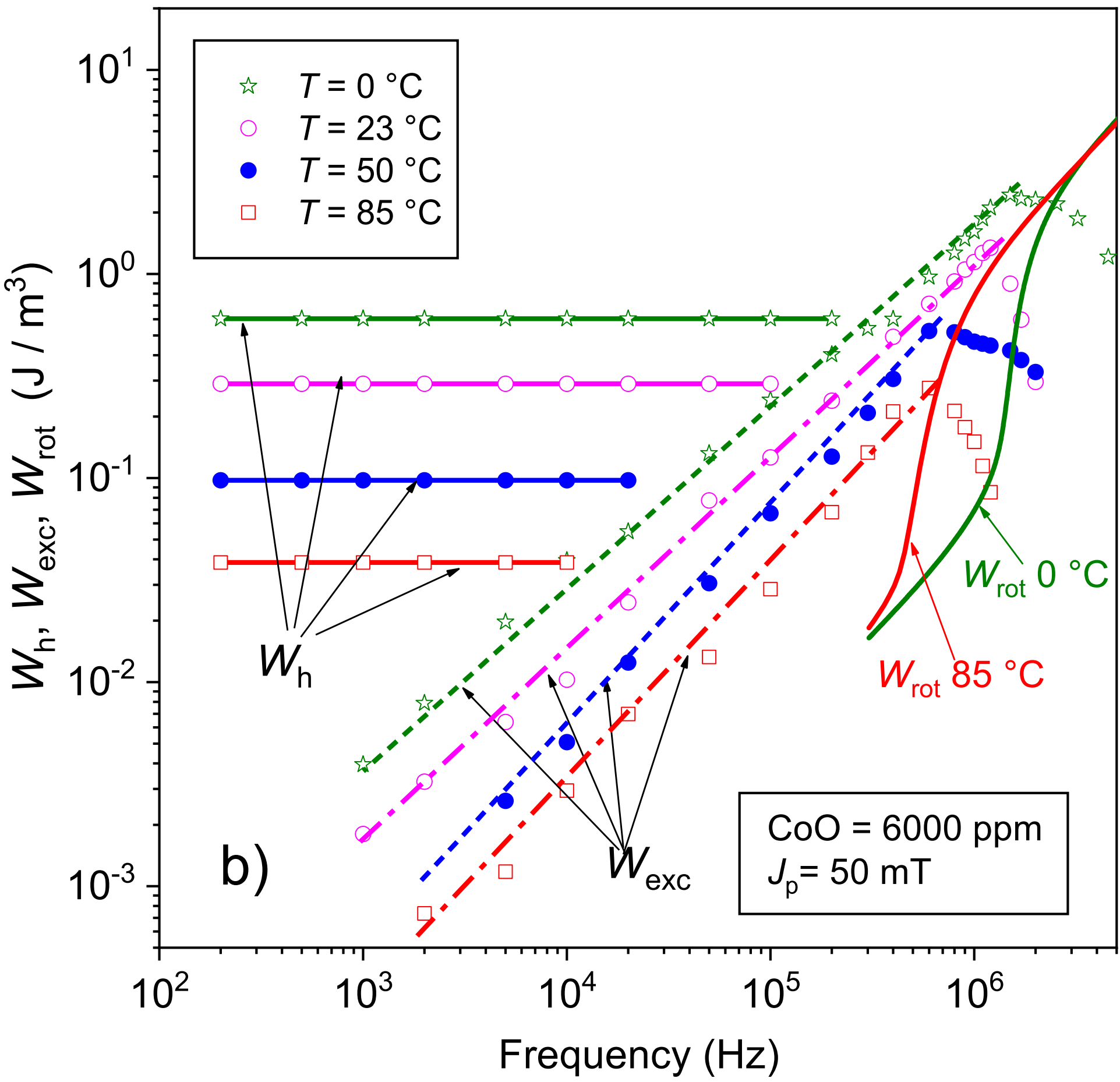

Journal of Applied Physics

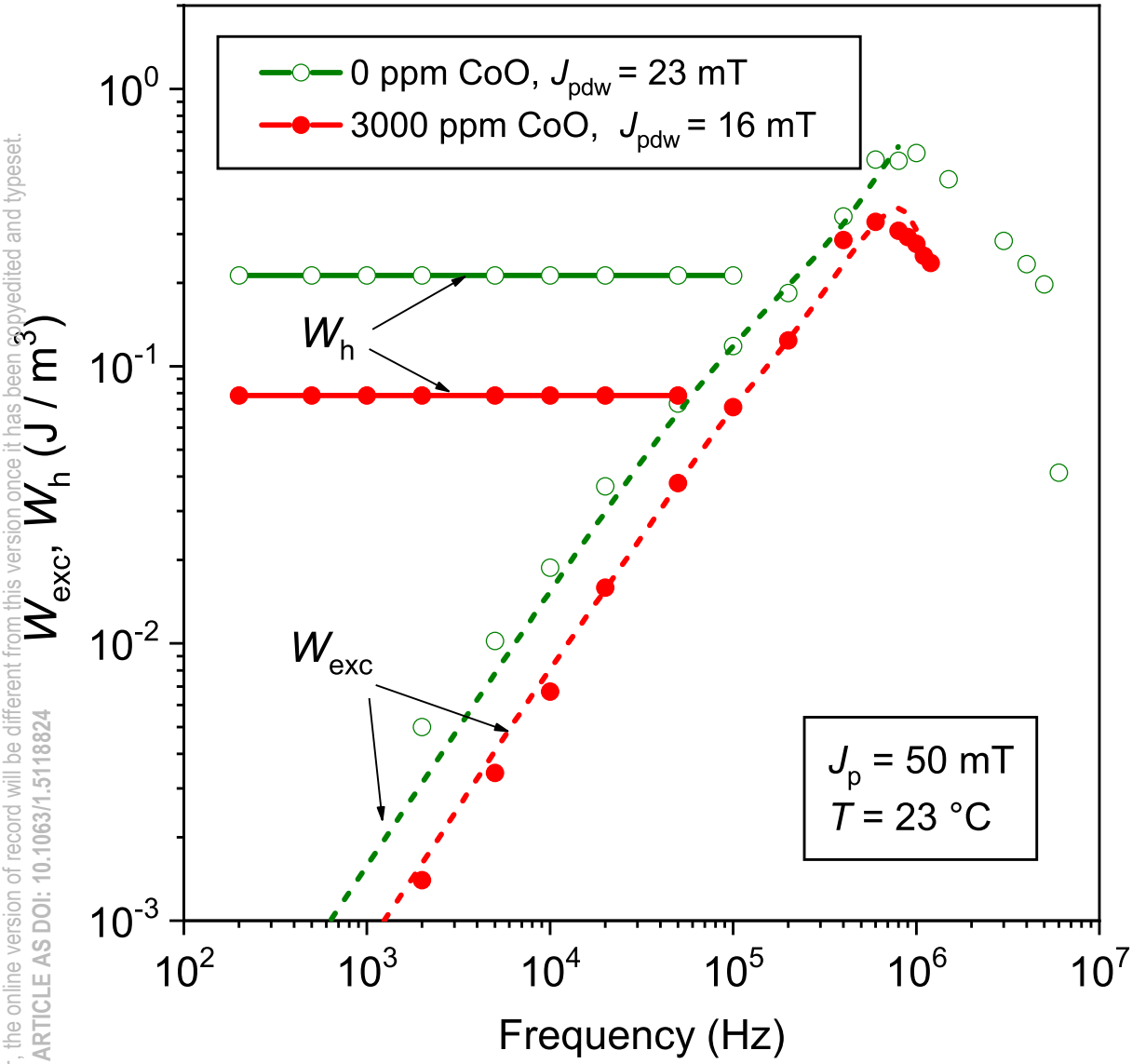

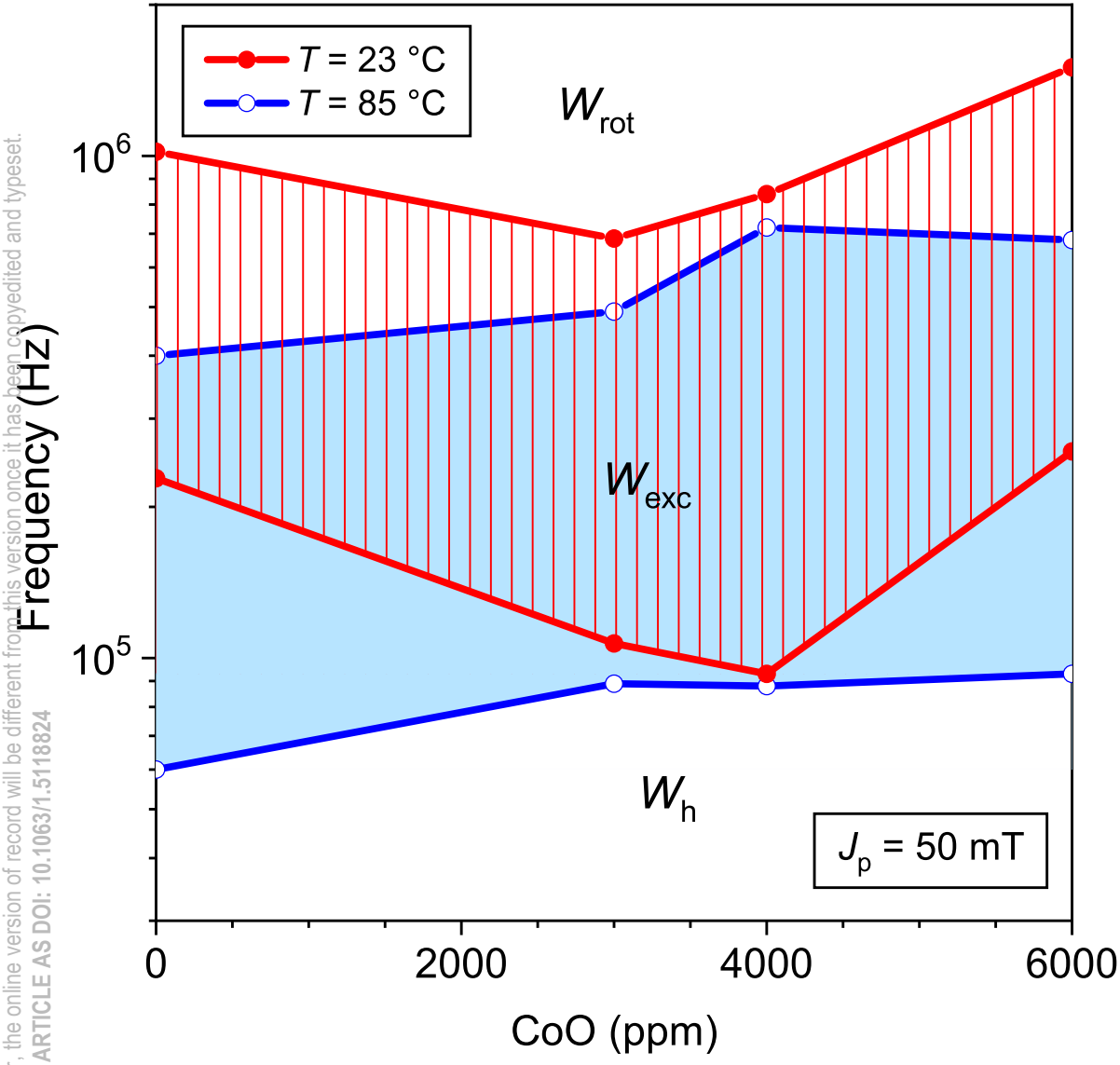

Journal of Applied Physics

AIP Publishing